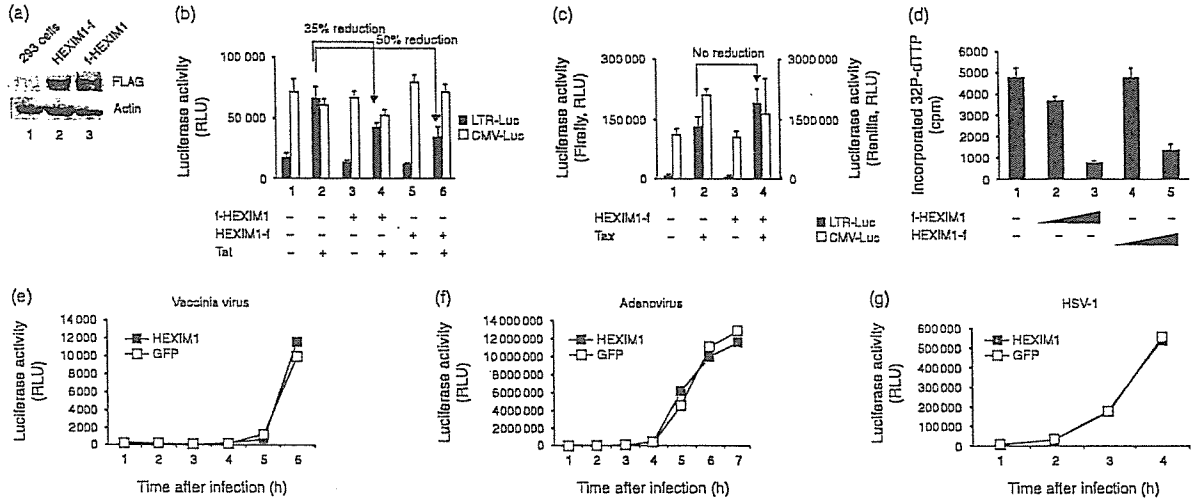

Fig. 1. Expression of hexamethylene bisacetamide-induced protein 1 (HEXIM1) specifically inhibits HIV-1 replication. (a) Detection of HEXIM1 cDNA tagged with a FLAG epitope at either the amino terminus (f-HEXIM1) or the carboxy terminus (HEXIM1-f) by western blot analysis in transiently transfected 293 cells (upper panel, approximately 65 kD). A western blot against actin is shown as a loading control (lower panel). (b) Expressing FLAG-tagged HEXIM1 decreased the luciferase activity driven by HIV-1 long terminal repeat (LTR) promoter in the presence of Tat (lanes 4 and 6, LTR-Luc, solid bars). However, FLAG-tagged HEXIM1 did not affect the expression of renilla luciferase from co-transfected plasmid driven by the cytomegalovirus (CMV) promoter (CMV-Luc, open bars). Representative data from three independent experiments done in triplicate are shown. Cells were transfected with 0.8 μg HEXIM1-expressing plasmid for the indicated lanes, 0.1 μg of pSV*tat* for the indicated lanes, and 0.1 μg of pLTR-Luc and 0.5 μg for phRL/CMV for all lanes. (c) Expressing FLAG-tagged HEXIM1 did not decrease the luciferase activity driven by HTLV-1 LTR promoter in the presence of Tax (lanes 2 and 4, LTR-Luc, solid bars) as well as renilla luciferase driven by the CMV promoter (CMV-Luc, open bars). Representative data from three independent experiments done in triplicate are shown. Cells were transfected with 0.8 μg of HEXIM1-expressing plasmid for the indicated lanes, 0.1 μg of pCGtax for the indicated lanes, and 0.1 μg of pHTLV LTR Luc and 0.5 μg for phRL/CMV for all lanes. (d) The dose-dependent reduction of HIV-1 production by transfection of HEXIM1-encoding plasmids (0.1 μg for lanes 2 and 4, 0.4 μg for lanes 3 and 5) along with a plasmid producing infectious HIV-1 (pNL4-3, 0.1 μg) in HeLa-CD4 cells. (e–g) Expressing HEXIM1-f did not limit the replication of vaccinia virus (e), adenovirus (f), or HSV-1 (g) in 293T cells. The *y*-axis represents the reporter gene activity, which reflects viral replication. Representative data from three independent experiments are shown. GFP, green fluorescent protein; RLU, relative light unit.

expression cassette, so that MLV vector-infected cells could be readily identified by the green fluorescence. Human T cell lines, including SUP-T1, MOLT-4, CEM, Jurkat, and M8166 were infected with MLV pseudotyped with vesicular stomatitis virus glycoprotein (VSV-G), and GFP-positive cells were collected with a FACS (Fig. 2a). For the negative control, we used MLV expressing GFP only. The successful introduction of HEXIM1-f into the cells was verified by RT-PCR and Western blot analysis (Fig. 2b and c). The total HEXIM1 protein expression in HEXIM1-f-transduced cells was approximately 3.7-, 1.5-, 2.0-, 4.8-, and 1.8-fold higher than in GFP-transduced cells in the CEM, Jurkat, MOLT-4, SUP-T1, and M8166 cell lines, respectively (Fig. 2c). To our surprise, the HEXIM1-f-expressing T cell lines remained GFP-positive, and therefore HEXIM1-f-positive, for more than 6 months and proliferated at rates almost indistinguishable from GFP-expressing cells. The expression levels of cyclin T1, cyclin T2, actin, and Bip/GRK78 in HEXIM1-f-expressing cells were almost identical to those in GFP-expressing cells, suggesting that the gene expression did not compensate the upregulated HEXIM1 (Fig. 2b and c). Expression of cyclin T2 was undetectable in M8166 cells (Fig. 2c). Similarly, HEXIM1-f expression did not affect the cell surface levels of the HIV-1 receptors CD4 and CXCR4 as demonstrated by FACS analysis (data not shown). These data indicate that the expression of HEXIM1-f did not reach levels where the physiological regulation of P-TEFb blocked cellular gene transcription.

The replication kinetics of HIV-1 or SIV was monitored by measuring the accumulation of viral capsid antigen in the culture medium. Strikingly, HIV-1 replicated more slowly in cells of all four T cell lines expressing HEXIM1-f than in cells expressing GFP (Fig. 2d–g). Similarly, HEXIM1-f-expressing M8166 cells supported SIV replication less efficiently than did GFP-expressing M8166 cells (Fig. 2h). Interestingly, the magnitude of HIV-1 replication delay was the most substantial in SUP-T1 cells, in which the levels of endogenous HEXIM1 were the lowest among the four cell lines tested for HIV-1 replication (Fig. 2c). Similar observations were made when the HIV-1 infection experiments were repeated,

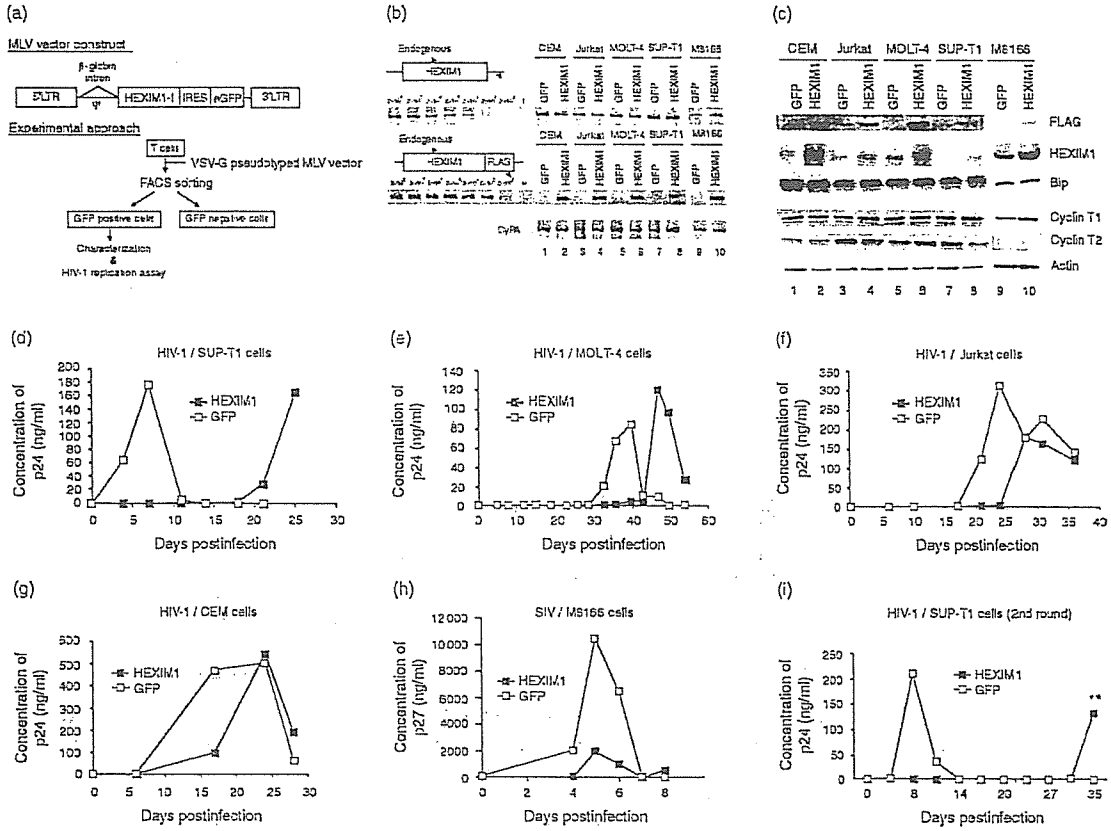

Fig. 2. Lentiviral replication is inhibited in various T cell lines constitutively expressing hexamethylene bisacetamide-induced protein 1 (HEXIM-1) cDNA tagged with a FLAG epitope at the carboxy terminus (HEXIM1-f). (a) The genomic organization of the retroviral vector expressing HEXIM1-f and a schematic representation of the experimental approach. (b) Detection of endogenous HEXIM1 and murine leukemia virus (MLV)-transduced HEXIM1-f (exogenous) mRNA by reverse transcriptase-polymerase chain reaction in green fluorescent protein (GFP)- and HEXIM1-f-expressing cells. The primer design is drawn schematically. Amplification efficiency was examined by using a known number of templates as standards for HEXIM1. Cyclophilin A (CyPA) was amplified to ensure the quality of the RNA. (c) Western blot analysis demonstrating expression of HEXIM1-f (denoted FLAG), endogenous HEXIM1 (HEXIM1), Bip, cyclin T1, cyclin T2, and actin in isolated T cell lines. (d–g) Replication profiles of HIV-1 (HXB2) in SUP-T1 (d), MOLT-4 (e), Jurkat (f), and CEM (g) cells either expressing HEXIM1-f or GFP alone. Representative data from two or three independent experiments are shown. (h) Replication profile of SIV in M8166 cells either expressing HEXIM1-f or GFP alone. Representative data from two independent experiments are shown. (i) The replication profiles of HIV-1 recovered from SUP-T1/HEXIM1-f cells (asterisk in Fig. 2d) in fresh SUP-T1/GFP or SUP-T1/HEXIM1-f. LTR, long terminal repeat.

indicating that the expression of functional HEXIM1-f did not change over the course of the replication monitoring. We tested whether the viruses emerged in HEXIM1-f-expressing cells were 'revertants' that might be able to replicate in HEXIM1-f-expressing cells as fast as in GFP-expressing cells. To address this, we recovered virus-containing culture supernatants from SUP-T1/HEXIM1-f cells at the peak of replication kinetics (asterisk, Fig. 2d). Then, both fresh SUP-T1/GFP and SUP-T1/HEXIM1-f were infected with the recovered virus and the replication kinetics was monitored. However, HIV-1 still replicated in SUP-T1/HEXIM1-f cells more slowly than in SUP-T1/GFP cells (Fig. 2i), akin to the original profiles (Fig. 2d), and the nucleotide sequences of LTR and *tat*, the primary targets of HEXIM1, remained unchanged (double asterisk in Fig. 2i). In addition, no mutations were found in viruses propagated in GFP-expressing SUP-T1 cells. Similar observations were made in MOLT-4 cells (data not shown). These data provide direct evidence that the expression of HEXIM1 inhibits lentiviral replication in human T cell lines.

Based on our experimental observations as well as the reported functions of HEXIM1, we assumed that the ability of HEXIM1 to limit HIV-1 replication was mostly due to the inhibition of Tat/P-TEFb-dependent transcriptional elongation. However, it was possible that HEXIM1 might also have targeted other viral replication steps. To test this possibility, we examined the viral entry and production processes separately. The efficiency of viral entry was analyzed by measuring the efficiency of

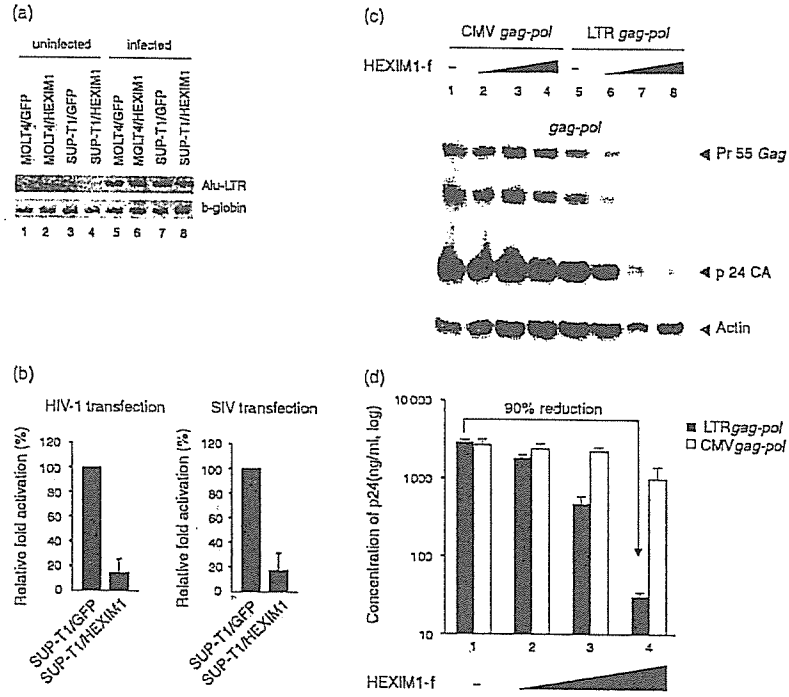

Fig. 3. Hexamethylene bisacetamide-induced protein 1 (HEXIM1) cDNA tagged with a FLAG epitope at the carboxy terminus (HEXIM1-f) does not affect the efficiency of viral integration or post-translational processes. (a) The Alu-long terminal repeat (LTR) and beta-globin polymerase chain reaction products from VSV-G-pseudotyped HIV-1-infected MOLT-4 and SUP-T1 cells expressing either green fluorescent protein (GFP) or HEXIM1-f alone were separated in an agarose gel and photographed. (b) The luciferase activities in SUP-T1/GFP or SUP-T1/HEXIM1-f cells electroporated with 10 μg of a plasmid encoding LTR-driven firefly luciferase plus 1 μg of phRL/cytomegalovirus (CMV). The firefly luciferase activity normalized to renilla luciferase activity in SUP-T1/GFP cells was set to 100%. The error bars represent the standard deviation of three independent experiments. (c) Western blot analysis showing Gag and its cleaved products expressed from either CMV promoter- or LTR promoter-driven *gag-pol* expression plasmid in the presence of pSVtat (0.1 μg, all lanes) and increasing amounts of HEXIM1-f (0.2 μg for lanes 2 and 6, 0.6 μg for lanes 3 and 7, and 2.0 μg for lanes 4 and 8). (d) The amount of p24 produced in the culture supernatant from cells analyzed in Fig. 3c was measured by enzyme-linked immunosorbent assay. Representative data from three independent experiments done in triplicate are shown. SIV, simian immunodeficiency virus.

viral integration. SUP-T1/GFP or SUP-T1/HEXIM1-f cells were infected with a replication-incompetent HIV-1 vector pseudotyped with VSV-G that expresses luciferase upon successful infection. We conducted an Alu-LTR PCR assay to detect the integrated viral genome. PCR products were detected only from HIV-1-infected cells (Fig. 3a). The signal intensities of Alu-LTR PCR products from GFP- and HEXIM1-f-expersing cells were similar. To compare the efficiency of viral infection as well as transcription quantitatively, we employed a real time PCR technique. Some infected cells were collected for an Alu-LTR PCR assay to quantify the amount of integrated viral genome, and the rest were processed to measure the amount of viral transcript as well as the luciferase activity. The amount of Alu-LTR PCR product from SUP-T1/HEXIM1-f cells was 3.5- and 3.3-fold more to that from SUP-T1/GFP cells from two independent experiments, respectively (Table 1). These data suggest that the efficiency of viral integration was not inhibited in HEXIM1-f-expressing SUP-T1 cells. In contrast, the relative abundance of HIV-1 transcript expressed in SUP-T1/HEXIM1-f cells was substantially decreased to 0.03 and 2.9% relative to SUPT1/GFP cells (Table 1). Furthermore, the luciferase activities were 200-fold lower in SUP-T1/HEXIM1-f cells than in SUP-T1/GFP cells (Table 1). Similar data was obtained from MOLT-4 cells infected with HIV-1 pseudotyped with VSV-G (data not shown). The transfection of plasmids encoding reporter viral DNA can bypass the viral entry and make it possible to measure the effect of HEXIM1 on LTR-driven transcription and translation. Consistent with above data, transfecting pNL-Luc into SUP-T1/HEXIM1-f cells gave significantly lower luciferase activities than SUP-T1/GFP cells (Fig. 3b, left). Similar data were obtained using pSIVmac239ΔnefLuc (Fig. 3b, right). These data strengthen the possibility that HEXIM1 targets post-integration processes.

To test this further, we analyzed the efficiency of post-transcriptional processes with a transient transfection assay measuring the amount of Pr55 Gag, a viral gene product, and virus-like particles (VLPs) produced in the culture

Table 1. Effect of hexamethylene bisacetamide-induced protein 1 (HEXIM1) cDNA tagged with a FLAG epitope at the carboxy terminus (HEXIM1-f) on viral entry and transcription in SUP-T1 cells examined by quantitative real time polymerase chain reaction.

		Integrated HIV-1 genome			HIV-1 transcript			Luciferase activity	
Exp.	Transduced gene	Alu-LTR (copy)	β-globin (copy)	Normalized[a] (%)	HIV-1 RNA (copy)	CyPA (copy)	Normalized[b] (%)	RLU[c]	Normalized[d] (%)
1	GFP	5.2×10^5	6.7×10^6	100.0	1.6×10^6	6.8×10^7	100.0	3.2×10^5	100.0
	HEXIM1-f	2.0×10^6	7.4×10^6	351.3	6.7×10^1	1.0×10^8	0.03	1.5×10^3	0.5
2	GFP	4.6×10^6	1.8×10^7	100.0	3.1×10^8	8.9×10^7	100.0	7.1×10^5	100.0
	HEXIM1-f	1.6×10^7	1.9×10^7	333.2	9.4×10^6	9.3×10^7	2.9	3.4×10^3	0.5

[a]The number of Alu-long terminal repeat (LTR) products divided by the number of beta-globin products in SUP-T1/GFP is set to 100%. The abundance of Alu-LTR products in SUP-T1/HEXIM1-f relative to SUP-T1/green fluorescent protein (GFP) is shown.
[b]The number of HIV-1 RNA transcripts in SUP-T1/GFP divided by the number of cyclophilin A (CyPA) transcripts is set to 100%. The abundance of HIV-1 RNA in SUP-T1/HEXIM1-f relative to SUP-T1/GFP is shown.
[c]The luciferase activity is shown by relative light unit (RLU).
[d]The luciferase activity in SUP-T1/GFP is set to 100%. The luciferase activity in SUP-T1/HEXIM1-f relative to SUP-T1/GFP is shown.

supernatants. For this purpose, we used the CMV promoter-driven *gag-pol* expression plasmid, because HEXIM1-f did not affect CMV-driven transcription (Fig. 1b). At the levels of HEXIM1-f where LTR-driven Tat-dependent transcription was drastically inhibited (Fig. 3c, lanes 7, 8), the amount of CMV promoter-driven Gag expression was almost identical to that in the absence of HEXIM1-f (Fig. 3c, lanes 1–4). Furthermore, the processing pattern of Pr55 Gag in the presence of HEXIM1-f was identical to that in its absence (Fig. 3c). These data indicate that HEXIM1-f did not inhibit the transcription from a Tat-independent promoter, the translation of viral protein, or the protease activity of HIV-1. Finally, the potential effect of HEXIM1 on viral budding was examined. To do this, the amount of p24 CA in the culture supernatant of transfected cells was quantified as a representation of the amount of VLP. Expressing HEXIM1-f reduced VLP production from cells co-transfected with pLTR*gag-pol* and pSVtat at levels comparable to the protein expression levels (Fig. 3c and d). In contrast, expressing HEXIM1-f did not reduce the amount of VLP produced by cells co-transfected with pCMV*gag-pol* and pSVtat in conditions in which Tat-dependent LTR transcription was substantially inhibited (Fig. 3c and d). Taken together, this indicates that HEXIM1-f lowers the efficiency of Tat-dependent transcription from LTR promoter but does not block the efficiency of the late phase of the viral life cycle including translation, Gag's assembly, and budding. Thus, it is likely that HEXIM1 primarily targets Tat/P-TEFb-dependent transcription to inhibit HIV-1 replication.

Our findings demonstrated that HEXIM1, a cellular P-TEFb inhibitor, is a specific negative regulator of lentiviral replication in human T cell lines. The replication of vaccinia virus, adenovirus, and HSV-1 were not affected by HEXIM1-f expression; however, the *tat*-dependent transcription of the LTR promoter of both HIV-1 and SIV was reduced by HEXIM1-f. HEXIM1 limited replication of HIV-1 dramatically at levels where it did not visibly affect cell physiology (as little as a 5-fold increase over the endogenous levels), nor were revertants immediately selected in HEXIM1-f-expressing cells. These data support the feasibility of developing HIV-1 inhibitors targeting the processes in which HEXIM1 is involved. For example, it is conceivable to hunt for a non-toxic chemical inducer for HEXIM1 since expression of HEXIM1 is induced by hexamethylene bisacetamide (HMBA) that is considerably toxic for cells [20].

P-TEFb has been shown to support transcription of the *c-myc* and CIITA transcription factors (reviewed in [21,22]). The functions of these transactivators are critical for cell proliferation, but in this study constitutive expression of HEXIM1-f, which reduces P-TEF-b activity, did not affect the cell proliferation of human T cell lines, the human epithelial cell lines HEK293 or the NP2 glioblastoma cell lines (data not shown). How can this be explained? Very recently, a high-molecular-weight bromodomain protein, Brd4, was found to function as a 'cellular *tat*' [23,24]. Interestingly, it was shown that Brd4 binds not only to cyclin T1 but also to cyclin T2, a widely expressed variant of cyclin T, to which HEXIM1 binds but Tat does not [23–25]. We hypothesize that Brd4 might be able to recruit and activate P-TEFb more efficiently than does Tat, leaving cellular transcription unaffected by the upregulated expression of HEXIM1 from the retroviral vector. An alternative possibility comes from the fact that HEXIM1 does not interact with the ubiquitously expressed cyclin K, which functions as a P-TEFb component. It is possible that Tat is not able to utilize P-TEFb consisting of CDK9 and cyclin K but Brd4 can, such that cyclin K may substitute for cyclin T1 to support Brd4-mediated cellular gene transcription.

Acknowledgements

We thank Dr. Tsutomu Murakami for the critical reading of the manuscript. This work was partly supported by Japan Health Science Foundation, Japanese Ministry of

Health, Labor and Welfare, and Japanese Ministry of Education, Culture, Sports, Science and Technology.

Sponsorship: This work was partly supported by Japan Health Science Foundation, Japanese Ministry of Health, Labor and Welfare, and Japanese Ministry of Education, Culture, Sports, Science and Technology.

References

1. Marshall N, Price D. **Control of formation of two distinct classes of RNA polymerase II elongation complexes.** *Mol Cell Biol* 1992; 12:2078–2090.
2. Kuiken C, Foley B, Hahn B, Korber B, Marx P, McCutchan F, *et al.*, editors. *HIV Sequence Compendium 2000.* Los Alamos: Theoretical Biology and Biophysics Group, Los Alamos National Laboratory, 2000.
3. Barboric M, Peterlin BM. **A new paradigm in eukaryotic biology: HIV Tat and the control of transcriptional elongation.** *PLoS Biol* 2005; 3:e76.
4. Nguyen V, Kiss T, Michels A, Bensaude O. **7SK small nuclear RNA binds to and inhibits the activity of CDK9/cyclin T complexes.** *Nature* 2001; 414:322–325.
5. Yang Z, Zhu Q, Luo K, Zhou Q. **The 7SK small nuclear RNA inhibits the CDK9/cyclin T1 kinase to control transcription.** *Nature* 2001; 414:317–322.
6. Li Q, Price J, Byers S, Cheng D, Peng J, Price D. **Analysis of the large inactive P-TEFb complex indicates that it contains one 7SK molecule, a dimer of HEXIM1 or HEXIM2, and two P-TEFb molecules containing Cdk9 phosphorylated at threonine 186.** *J Biol Chem* 2005; 280:28819–28826.
7. Michels A, Nguyen V, Fraldi A, Labas V, Edwards M, Bonnet F, *et al.* **MAQ1 and 7SK RNA interact with CDK9/cyclin T complexes in a transcription-dependent manner.** *Mol Cell Biol* 2003; 23:4859–4869.
8. Yik J, Chen R, Pezda A, Samford C, Zhou Q. **A human immunodeficiency virus type 1 Tat-like arginine-rich RNA-binding domain is essential for HEXIM1 to inhibit RNA polymerase II transcription through 7SK snRNA-mediated inactivation of P-TEFb.** *Mol Cell Biol* 2004; 24:5094–5105.
9. Barboric M, Kohoutek J, Price J, Blazek D, Price D, Peterlin B. **Interplay between 7SK snRNA and oppositely charged regions in HEXIM1 direct the inhibition of P-TEFb.** *EMBO J* 2005; 24:4291–4303.
10. Schulte A, Czudnochowski N, Barboric M, Schonichen A, Blazek D, Peterlin B, Geyer M. **Identification of a cyclin T-binding domain in Hexim1 and biochemical analysis of its binding competition with HIV-1 Tat.** *J Biol Chem* 2005; 280:24968–24977.
11. Fraldi A, Varrone F, Napolitano G, Michels A, Majello B, Bensaude O, Lania L. **Inhibition of Tat activity by the HEXIM1 protein.** *Retrovirology* 2005; 2:42.
12. Michels A, Fraldi A, Li Q, Adamson T, Bonnet F, Nguyen V, *et al.* **Binding of the 7SK snRNA turns the HEXIM1 protein into a P-TEFb (CDK9/cyclin T) inhibitor.** *EMBO J* 2004; 23:2608–2619.
13. Komano J, Miyauchi K, Matsuda Z, Yamamoto N. **Inhibiting the Arp2/3 complex limits infection of both intracellular mature vaccinia virus and primate lentiviruses.** *Mol Biol Cell* 2004; 15:5197–5207.
14. Wagner R, Graf M, Bieler K, Wolf H, Grunwald T, Foley P, Uberla K. **Rev-independent expression of synthetic gag-pol genes of human immunodeficiency virus type 1 and simian immunodeficiency virus: implications for the safety of lentiviral vectors.** *Hum Gene Ther* 2000; 11:2403–2413.
15. Masuda T, Planelles V, Krogstad P, Chen I. **Genetic analysis of human immunodeficiency virus type 1 integrase and the U3 att site: unusual phenotype of mutants in the zinc finger-like domain.** *J Virol* 1995; 69:6687–6696.
16. Willey R, Smith D, Lasky L, Theodore T, Earl P, Moss B, *et al.* **In vitro mutagenesis identifies a region within the envelope gene of the human immunodeficiency virus that is critical for infectivity.** *J Virol* 1988; 62:139–147.
17. Butler SL, Hansen MS, Bushman FD. **A quantitative assay for HIV DNA integration in vivo.** *Nat Med* 2001; 7:631–634.
18. Graf Einsiedel H, Taube T, Hartmann R, Wellmann S, Seifert G, Henze G, Seeger K. **Deletion analysis of p16(INKa) and p15(INKb) in relapsed childhood acute lymphoblastic leukemia.** *Blood* 2002; 99:4629–4631.
19. Zhou M, Lu H, Park H, Wilson-Chiru J, Linton R, Brady JN. **Tax interacts with P-TEFb in a novel manner to stimulate human T-lymphotropic virus type 1 transcription.** *J Virol* 2006; 80: 4781–4791.
20. Kusuhara M, Nagasaki K, Kimura K, Maass N, Manabe T, Ishikawa S, *et al.* **Cloning of hexamethylene-bis-acetamide-inducible transcript, HEXIM1, in human vascular smooth muscle cells.** *Biomed Res* 1999; 20:273–279.
21. Price DH. **P-TEFb, a cyclin-dependent kinase controlling elongation by RNA polymerase II.** *Mol Cell Biol* 2000; 20:2629–2634.
22. Garriga J, Grana X. **Cellular control of gene expression by T-type cyclin/CDK9 complexes.** *Gene* 2004; 337:15–23.
23. Jang M, Mochizuki K, Zhou M, Jeong H, Brady J, Ozato K. **The bromodomain protein Brd4 is a positive regulatory component of P-TEFb and stimulates RNA polymerase II-dependent transcription.** *Mol Cell* 2005; 19:523–534.
24. Yang Z, Yik J, Chen R, He N, Jang M, Ozato K, Zhou Q. **Recruitment of P-TEFb for stimulation of transcriptional elongation by the bromodomain protein Brd4.** *Mol Cell* 2005; 19:535–545.
25. Napolitano G, Licciardo P, Gallo P, Majello B, Giordano A, Lania L. **The CDK9-associated cyclins T1 and T2 exert opposite effects on HIV-1 Tat activity.** *AIDS* 1999; 13:1453–1459.

Antiviral Chemistry & Chemotherapy 17:167–174

Rapid propagation of low-fitness drug-resistant mutants of human immunodeficiency virus type 1 by a streptococcal metabolite sparsomycin

Kosuke Miyauchi, Jun Komano*, Lay Myint, Yuko Futahashi, Emiko Urano, Zene Matsuda, Tomoko Chiba, Hideka Miura, Wataru Sugiura and Naoki Yamamoto

AIDS Research Center, National Institute of Infectious Diseases, Toyama, Shinjuku, Tokyo, Japan

*Corresponding author: Tel: +81 3 5285 1111; Fax: +81 3 5285 5037; E-mail: ajkomano@nih.go.jp

Here we report that sparsomycin, a streptococcal metabolite, enhances the replication of HIV-1 in multiple human T cell lines at a concentration of 400 nM. In addition to wild-type HIV-1, sparsomycin also accelerated the replication of low-fitness, drug-resistant mutants carrying either D30N or L90M within HIV-1 protease, which are frequently found mutations in HIV-1-infected patients on highly active antiretroviral therapy (HAART). Of particular interest was that replication enhancement appeared profound when HIV-1 such as the L90M-carrying mutant displayed relatively slower replication kinetics. The presence of sparsomycin did not immediately select the fast-replicating HIV-1 mutants in culture. In addition, sparsomycin did not alter the 50% inhibitory concentration (IC_{50}) of antiretroviral drugs directed against HIV-1 including nucleoside reverse transcriptase inhibitors (lamivudine and stavudine), non-nucleoside reverse transcriptase inhibitor (nevirapine) and protease inhibitors (nelfinavir, amprenavir and indinavir). The IC_{50}s of both zidovudine and lopinavir against multidrug resistant HIV-1 in the presence of sparsomycin were similar to those in the absence of sparsomycin. The frameshift reporter assay and Western blot analysis revealed that the replication-boosting effect was partly due to the sparsomycin's ability to increase the –1 frameshift efficiency required to produce the *Gag–Pol* transcript. In conclusion, the use of sparsomycin should be able to facilitate the drug resistance profiling of the clinical isolates and the study on the low-fitness viruses.

Keywords: drug resistant mutants, enhancement of replication, HIV-1, low-fitness mutants, sparsomycin

Introduction

Highly active antiretroviral therapy (HAART) has been successful in controlling the progression of AIDS caused by HIV-1. However, HAART has accelerated the emergence and spread of multidrug-resistant HIV-1. Once drug-resistant HIV-1 occurs in a HIV-1-infected patient, the success rate of HAART drops substantially. Resistance testing has been shown to be valuable to optimize HAART against HIV-1 infection (Hirsch *et al.*, 2000; Rodriguez-Rosado *et al.*, 1999). Profiling drug resistance might be necessary even before the initiation of HAART because of the spread of drug-resistant HIV-1 (Boden *et al.*, 1999; Gehringer *et al.*, 2000; Yerly *et al.*, 1999).

Genotypic and phenotypic resistance testing are the two major ways to determine the drug resistance of clinical HIV-1 isolates. For genotyping, the HIV-1 genome isolated from the infected individuals is sequenced. This HIV-1 genome is than cross-referenced with a database and we are able to predict the drug resistance profile of HIV-1. However, it is impossible to predict the phenotype when we encounter a combination of mutations that has never been documented. This may raise a concern when a new drug is released in the market. Another problem in the genotyping is the presence of genotype-phenotype discordance (Parkin *et al.*, 2003; Sarmati *et al.*, 2002).

Alternatively, for the phenotypic resistance testing, the drug resistance profiles are measured by many biological/virological assay systems (Hertogs *et al.*, 1998; Iga *et al.*, 2002; Jarmy *et al.*, 2001; Kellam & Larder, 1994; Menzo *et al.*, 2000; Walter *et al.*, 1999). Phenotypic resistance testing is powerful because the diagnosis is based on experimental observations. Among the systems, ones that depend on the multi-round HIV-1 replication seemed to provide the best drug resistance data reflecting the *in vivo* condition. However, many drug-resistant mutants have lower replication capabilities than wild-type (wt) HIV-1, which makes the phenotypic resistance testing difficult and time-consuming. In order to overcome these problems, it would be useful to develop a technique to make HIV-1

replicate faster without altering the effectiveness of antiretroviral compounds.

During our search for an inhibitor of HIV-1 replication, we found sparsomycin, a metabolite from *Streptomyces sparsogenes*, which reproducibly enhanced the replication of HIV-1. Therefore, we tested whether sparsomycin merits phenotypic drug resistance profiling studies on low-fitness HIV-1 isolates.

Materials and methods

Cells and viruses

Human embryonic kidney (HEK) 293T cells were maintained in Dulbecco's modified Eagle's medium (Sigma-Aldrich, Tokyo, Japan) supplemented with 10% fetal bovine serum (FBS; Hyclone, Logan, UT, USA), penicillin and streptomycin (Invitrogen, Carlsbad, CA, USA). H9, Jurkat, SupT1 and HPB-Ma cells were maintained in RPMI1640 (Sigma-Aldrich) supplemented with 10% FBS, penicillin and streptomycin. All the cell lines were incubated at 37°C in a humidified 5% CO_2 atmosphere. As previously described, HIV-1 (HXB2) was produced by transfecting proviral DNA into 293T cells and collecting the culture medium 3 days post-transfection (Komano *et al.*, 2004). The replication-incompetent HIV-1 (HXB2 Δ*vpr*, Δ*rev*, Δ*env*, Δ*nef*) was produced by transfecting the proviral DNA carrying renilla luciferase with the *nef* open reading frame into 293T cells, along with the expression plasmid for *env*, *tat*, *rev* and *nef* (pIIIex) as described previously in Komano *et al.* (2004). As previously described, the D30N, L90M, and D25N protease mutants of HIV-1 were generated by the site-directed mutagenesis (Sugiura *et al.*, 2002). The multidrug-resistant HIV-1 DR3577 was a clinical isolate from a patient on HAART in which reverse transciptase carried the following mutations M41L, D67N, K70R, V75M, K101Q, T215F and K219Q and protease carried the following mutations L10I, K20R, M36I, M46I, L63P, A71V, V82T, N88S and L90M. For the generation of replication-incompetent murine leukaemia virus (MLV) vector expressing firefly luciferase, pCMMP luciferase was transfecting into 293T cells along with *gag/pol* and VSV-G expressing plasmids as described previously (Komano *et al.*, 2004).

Chemical compound

Sparsomycin was either purchased from Sigma-Aldrich (cat. S1667) or obtained from Dr Nakajima (Toyama Prefectural University, Toyama, Japan). Sparsomycin was dissolved in 2mM dimethyl sulphoxide and stored at –20°C until use.

Monitoring HIV-1 replication

For HIV-1 infection, 1×10^6 cells were incubated with the culture supernatant containing approximately 10 ng of p24. Alternatively, wt HIV-1, or D30N and L90M mutants were introduced into cells either by electroporation or DEAE-dextran-mediated protocol as previously described (Matsuda *et al.*, 1993; Miyauchi *et al.*, 2005). The culture supernatants were collected everytime the infected cells were split until they ceased to proliferate. The amount of p24 antigen of HIV-1 in the culture supernatants was quantified by using Retro TEK p24 antigen ELISA kit according to the manufacturer's protocol (Zepto Metrix, Buffalo, NY, USA). The signal was detected by Vmax ELISA reader (Molecular Devices, Palo Alto, CA, USA).

Determining 50% inhibitory concentrations (IC_{50})

IC_{50} was calculated by using a reporter cell line, MARBLE, developed by Sugiura *et al.* (personal communication). In brief, a clone of HPB-Ma carrying the long terminal repeat (LTR)-driven firefly luciferase cassette integrated in its genome was infected with HIV-1 and incubated in the presence of varying concentrations of antiretroviral compounds for a week. The cells were then lysed to measure the firefly luciferase activity, which represented the propagation of HIV-1 in culture. The firefly luciferase activity was normalized by constitutively-expressed renilla luciferase activity. The dual luciferase assay was performed according to the manufacturer's protocol (Promega, Madison, WI, USA). Chemiluminescence was detected by Lmax (Molecular Devices).

Reporter assay

The –1 frameshift reporters, pLuc (–1) and pLuc (0), were kindly provided by Dr Brakier-Gingras (Dulude *et al.*, 2002). The renilla luciferase expression vector phRL/CMV was purchased from Promega. pLTR Luc encoded GFP-luciferase under the regulation of HIV-1's LTR promoter (Komano *et al.*, 2004). pLTRΔnefLuc encoded renilla luciferase by substituting *nef* in the proviral context of HXB2 (Komano *et al.*, 2004). Plasmids were transfected into 293T cells by Lipofectamine 2000 plus reagent in accordance with the manufacturers' protocol (Invitrogen). For the detection of luciferase activities, the dual glo luciferase assay was performed at 2–3 days post-transfection or post-infection according to the manufacturers' protocol (Promega). The signal was detected by Vmax ELISA reader (Molecular Devices).

Western blot analysis

COS-7 cells were transfected with Lipofectamine 2000 (Invitrogen) or Fugen6 (Roche, Basel, Switzerland) according to the manufacturer's protocol with proviral DNA encoding the D25N protease mutant. At 48 h post-transfection, cells were washed with PBS and lysed in a buffer containing 4% SDS, 100 mM Tris-HCl (pH 6.8), 12% 2-ME, 20% glycerol and bromophenol blue.

Samples were boiled for 10 min. Protein lysates approximately equivalent to 5×10^4 cells were separated in 5–20% SDS-PAGE (Perfect NT Gel, DRC, Tokyo, Japan), transferred to a polyvinylidene fluoride (PVDF) membrane (Immobilon-P^{SQ}; Millipore, Billerica, MA, USA), and blocked with 5% dried non-fat milk (Yuki-Jirushi, Tokyo, Japan) in PBS. For the primary antibody, we used rabbit anti-*Gag* polyclonal antibody or mouse anti-*Gag* monoclonal antibody. For the secondary antibody, either a biotinylated anti-rabbit antibody or a biotinylated anti-mouse goat antibody (GE Healthcare Bio-Science, Piscataway, NJ, USA) was used. For the tertiary probe, a horseradish peroxidase-conjugated streptoavidin (GE Healthcare Bio-Science) was used. Signals were developed by incubating blots with a chemilumenescent horseradish peroxidase substrate (GE Healthcare Bio-Science) and detected by using Lumi-Imager F1 (Roche).

Results

The structure of sparsomycin, a metabolite from *Streptomyces sparsogenes*, is unique in that it comprises two unusual entities, a monooxodithioacetal moiety and a uracil acrylic acid moiety (Figure 1A). H9 cells were infected with HIV-1 and then maintained in the presence of varying concentrations of sparsomycin. Dimethyl sulphoxide was added in the absence of sparsomycin throughout this study. At 7 days post-infection, a massive syncytial formation was found in the presence of sparsomycin (Figure 1B). The higher the concentration of sparsomycin, the faster p24 accumulated in the culture supernatants (Figure 1C). Similar observations were made in Jurkat, SupT1 (Figures 1D and E), and HPB-Ma cells although the speed of p24 accumulation appeared different among the cell lines. On the other hand, sparsomycin did not show any detectable effect on the cell growth under concentrations of 500 nM.

These results could be due to sparsomycin's ability to either boost HIV-1 replication or select a mutant that replicated substantially faster than the wt HIV-1. To differentiate these possibilities, we recovered the virus-containing culture supernatants from the H9 cell culture at the peak of HIV-1 replication in the presence of 400 nM sparsomycin (asterisk in Figure 1F). Then fresh H9 cells were infected with the recovered virus, the cells were split into two samples and 400 nM of sparsomycin was added to each sample. If sparsomycin selected fast-growing mutants, the replication profiles of HIV-1 should resemble the original sample with sparsomycin (solid circle, Figure 1F) regardless of sparsomycin's presence. However, the replication profile in the presence of sparsomycin shifted leftward (Figure 1G), suggesting that it was unlikely that sparsomycin selected the fast-replicating viral mutants. Therefore, it is likely that sparsomycin boosted HIV-1 replication. Replication-enhancing effects were also seen by using the chemically-synthesized derivatives of sparsomycin (unpublished data; Nakajima *et al.*, 2003). The replication-boosting effect levelled-out at 500 nM, an approximately 20-fold lower concentration than the 50% toxic dose (TD_{50}) of sparsomycin (Ash *et al.*, 1984).

To demonstrate the usefulness of sparsomycin in HIV-1 research, we have examined whether sparsomycin can also boost the replication of drug-resistant low-fitness isolates. The D30N and L90M are common drug-resistant mutations found within HIV-1 protease in HIV-1-infected patients on HAART (Devereux *et al.*, 2001; Kantor *et al.*, 2002; Pellegrin *et al.*, 2002; Sugiura *et al.*, 2002). We introduced proviral DNA carrying the D30N or L90M mutation into H9, Jurkat, and SupT1 cells. HIV-1 replication was than monitored in the presence of 400 nM of sparsomycin. The replication of both viral mutants was substantially enhanced in the presence of sparsomycin in H9 cells (Figures 2A and B). The replication of the L90M-carrying mutant was also enhanced in Jurkat and SupT1 cells (Figures 2C and D). Of note, the replication enhancement appeared profound when HIV-1 displayed relatively slower replication kinetics (for example, the replication of D30N-carrying mutant versus the wt HIV-1 in H9 cells or the replication of HIV-1 in SupT1 versus H9 cells).

Considering the use of sparsomycin in the phenotypic resistance testing, it is critical to know whether sparsomycin affects HIV-1's sensitivity to the antiretroviral drugs. The respective IC_{50} of representative antiretroviral drugs in the absence and the presence of 400 nM sparsomycin were as follows: reverse transcriptase inhibitors; lamivudine, 13.7 and 10.4 nM, and stavudine, 6.3 and 17.0 nM; an non-nucleoside reverse transcriptase inhibitor, nevirapine, 78.2 and 146.4 nM; and protease inhibitors, nelfinavir, 2.8 and 1.0 nM, indinavir, 4.2 and 3.0 nM, and amprenavir, 3.4 and 3.3 nM. Then, we examined whether the presence of sparsomycin affected the IC_{50} of both zidovudine (AZT) and lopinavir (LPV) against a multidrug-resistant HIV-1 isolate, DR3577. The magnitude of both AZT and LPV-resistance of DR3577 was in the order of 2 log (data not shown). The IC_{50}s of AZT in the presence and absence of 400 nM sparsomycin were 14.0 and 36.7 nM, respectively, and for LPV they were 103.1 and 78.9 nM, respectively. These data suggested that the presence of sparsomycin did not significantly influence the IC_{50} of antiretroviral drugs on the replication of both wt and drug-resistant HIV-1.

Finally, we investigated the possible mechanisms that sparsomycin enhanced the replication of HIV-1 and its mutants although the estimated magnitude of enhancement per single replication cycle was small. To do this, we used non-T cells to increase the sensitivity of assays. First, we examined if the early phase of HIV-1's life cycle was

Figure 1. The enhancement of HIV-1 replication by sparsomycin

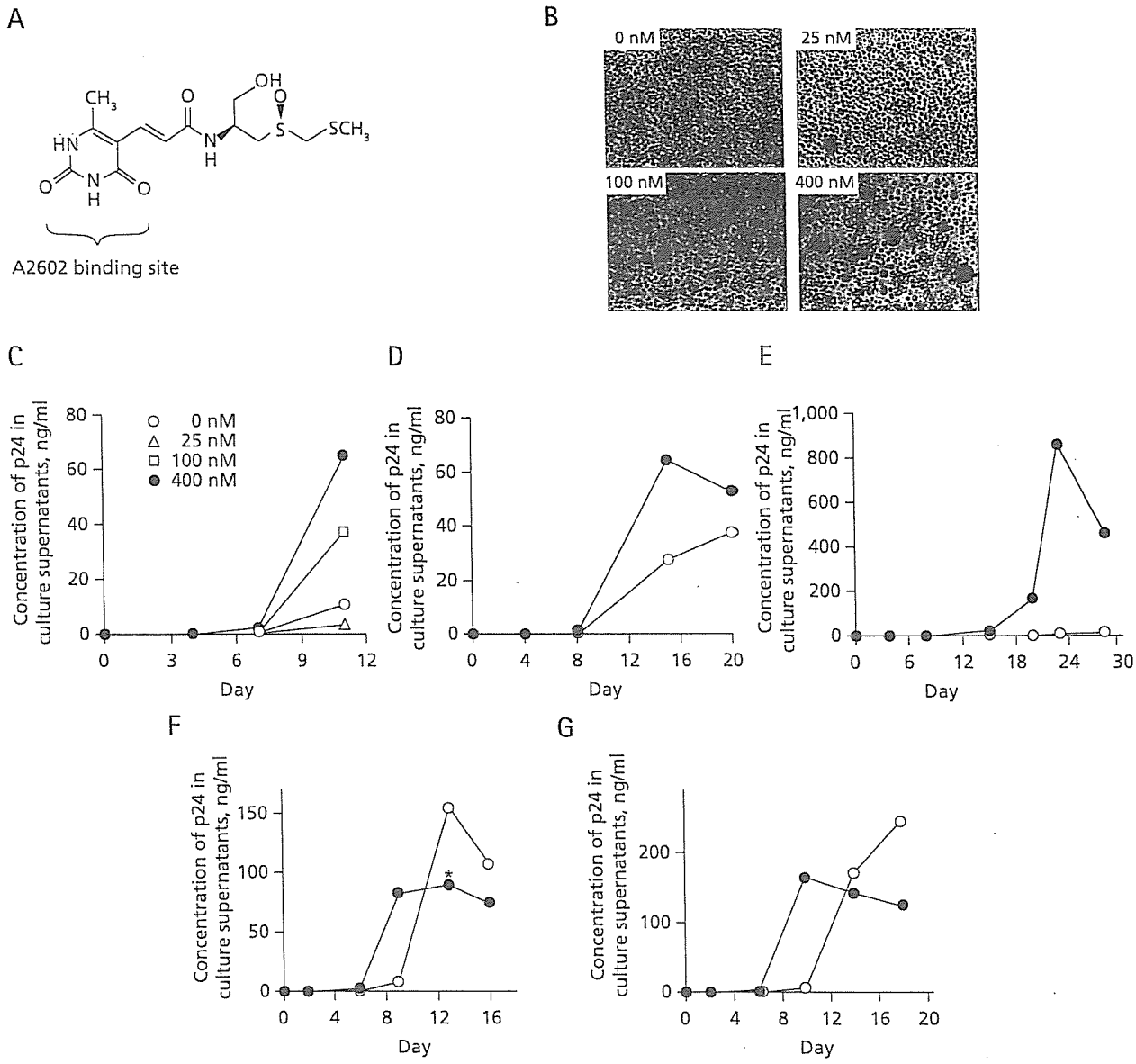

(A) Structure of sparsomycin. The uracil acrylic acid moiety confers the binding capacity to the conserved nucleobase A2602 of the large ribosomal subunit. (B) H9 cells infected with HIV-1 were photographed at a week after infection (magnification, ×200). (C) The replication profiles of HIV-1 in H9 cells in the presence of varying concentrations of sparsomycin. (D-G). The replication profiles of HIV-1 in Jurkat (D), SupT1 (E), and H9 cells (F and G) in the presence of sparsomycin (400 nM, solid circle) or in the absence (open circle; F and G). Virus-containing culture supernatant was collected at 13 days post-infection (asterisk, F) to infect fresh H9 cells and the replication profiles of HIV-1 were analysed in the presence of sparsomycin (400 nM, solid circle) or in the absence (open circle, G).

positively affected by sparsomycin. In the presence of increasing concentrations of sparsomycin, 293 CD4$^+$ T-cells and NP2 CD4 CXCR4 cells were infected with either a replication-deficient HIV-1 vector enveloped with its own *Env* or a VSV-G-psueodotyped MLV vector. Two days post-infection, cells were lysed to measure the luciferase activities representing the efficiency of viral infection. Our results indicate that luciferase activities were not significantly increased at the replication-enhancing dose for both HIV-1 and MLV vectors (Figure 3A). Thus suggesting that the early phase of the retroviral life cycle was not detectably affected by sparsomycin.

Figure 2. Sparsomycin's ability to enhance replication of low-fitness drug resistant HIV-1 mutants

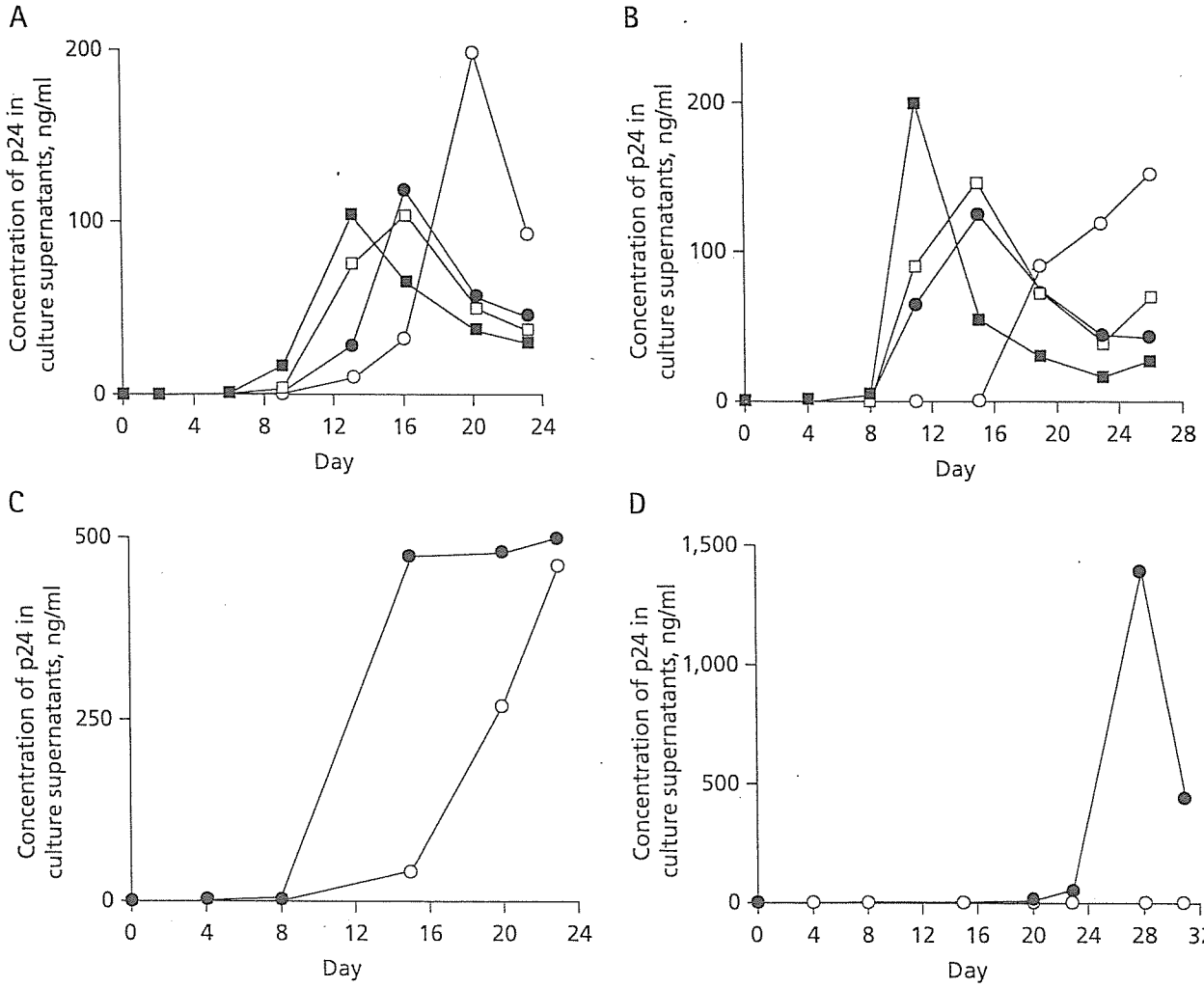

(A and B) The replication kinetics of the D30N-carrying (circle) and L90M-carrying (square) mutants in the presence of sparsomycin (400 nM, solid) or in the absence (open) were investigated twice independently in H9 cells. (C and D) The replication kinetics of the L90M-carrying mutant were examined in Jurkat cells (C) and SupT1 cells (D) in the presence of sparsomycin (400 nM, solid circle) or in the absence (open circle).

Next, we examined the possible active role of sparsomycin in the late phase of HIV-1's life cycle. Sparsomycin has been reported to be a potential enhancer of the −1 frameshift (Dinman *et al.*, 1997). Therefore, we tested whether sparsomycin could positively affect the efficiency of the translational −1 slip at HIV-1's frameshift signal using the reporter assay system established by Dulude *et al.* (2002). The −1 frameshift reporter was created by placing the firefly luciferase in the *pol* frame, pLuc(−1), whereas the control plasmid pLuc(0) has the luciferase in the *gag* frame after the frameshift signal (Figure 3B). In addition, HIV-1's LTR-driven luciferase reporter constructs were tested (pLTR Luc and pLTRΔnefLuc; Figure 3B). We transfected these reporter plasmids into 293T cells along with the renilla luciferase-expressing plasmid phRL/CMV (Promega) to measure the non-specific or toxic effects, if any, of sparsomycin. Cells were incubated in the presence of varying concentrations of sparsomycin for 3 days. Then the dual luciferase assay was performed. The pLuc(−1) behaved differently from the other groups in that the luciferase activities from the pLuc(−1) increased in a dose-dependent fashion. The magnitude of increasement was 2.3-fold at the replication-enhancing dose (Figure 3C). The positive correlation between the relative luciferase activity and the concentration of sparsomycin was statistically significant (r=0.926, P<0.001, n=8, Student's t-test). In contrast, the luciferase activities from the other reporters, even the renilla luciferase plasmid

co-transfected with the pLuc(-1) vector, remained unchanged (Figure 3C). These data suggested that sparsomycin positively affected the efficiency of HIV-1's –1 frameshift. It also suggested that sparsomycin did not enhance transcription from the viral promoter or the translation of proteins driven by the LTR promoter to enhance HIV-1 replication.

If the efficiency of –1 frameshift was increased, we would expect that the *Gag–Pol* to *Gag* ratio to increase. To test this, we transfected COS-7 cells with the HIV-1's proviral DNA carrying the D25N mutation in protease that produced catalytically inactive protease to increase the sensitivity of detecting *Gag–Pol* (Xie *et al.*, 1999). When sparsomycin was added, the intensities of *Gag–Pol* gradually increased in relation to the reporter assay. The *Gag–Pol* to *Gag* ratio reached 1.3-fold at 400 nM sparsomycin when normalized with results produced in the absence of sparsomycin (Figure 3D). The average and standard deviation of the *Gag–Pol* to *Gag* ratio from four independent experiments were 1.29 ± 0.14 at the replication enhancing concentration of sparsomycin (1.29-, 1.48-, 1.16-, and 1.24-fold increase). Similar results were obtained by using

Figure 3. The possible mechanism of HIV-1 replication enhancement by sparsomycin

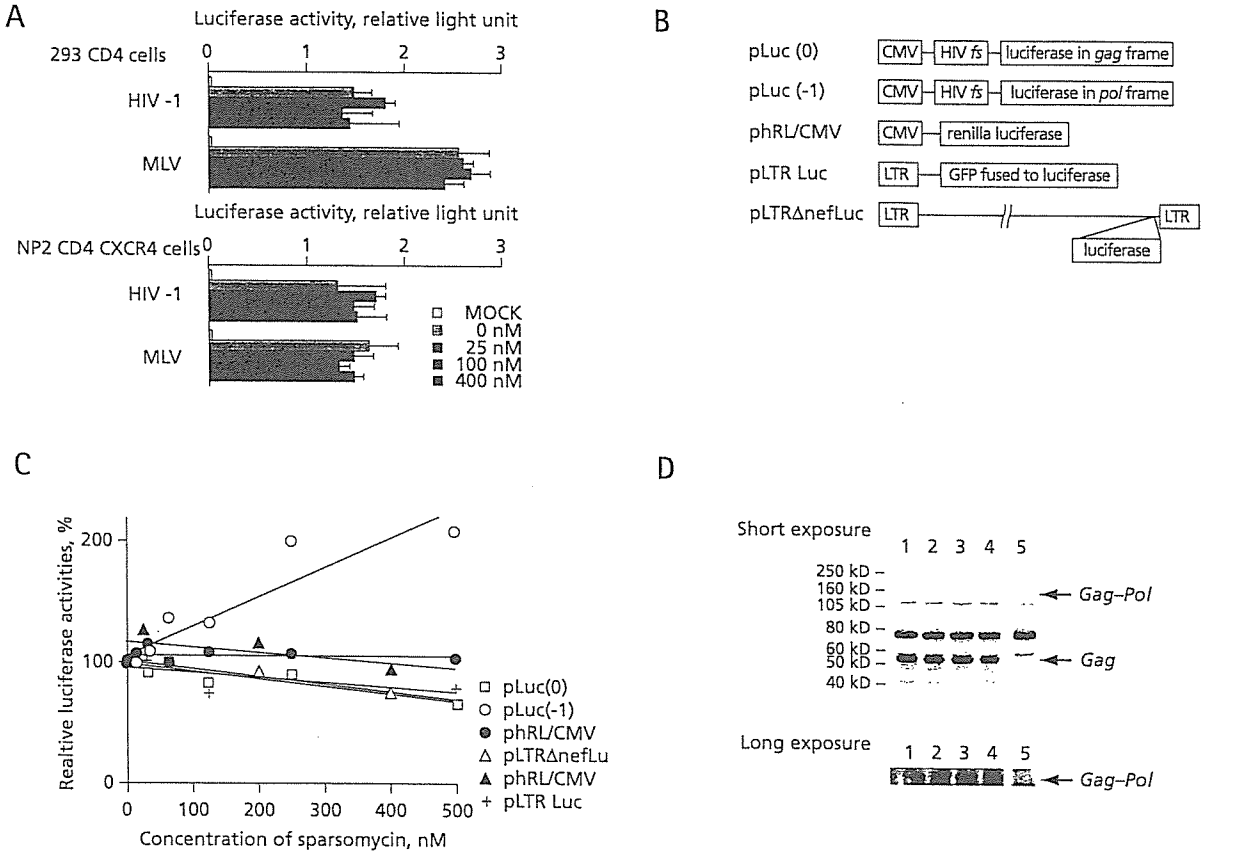

(A) The single round infection efficiencies of HIV-1 and murine lukaemia virus (MLV) vectors measured by the virally-encoded luciferase activities in 293 CD4⁺ T-cells and NP2 CD4 CXCR4 cells in the presence of varying concentrations of sparsomycin. **(B)** The schematic drawing of constructs used in the reporter assay. The HIV-1's frameshift signal (*fs*) was placed between the CMV promoter and the luciferase. The luciferase was placed in either the *gag* frame (pLuc(0)) or the *pol* frame (pLuc(-1)). The renilla luciferase expression vector phRL/CMV was used in parallel. The pLTR Luc encodes the GFP-luciferase driven by HIV-1's LTR promoter. The pLTRΔnefLuc has the renilla luciferase substituting *nef* in the proviral context of HXB2. **(C)** The luciferase activities from the above reporter constructs without sparsomycin were set as 100% and the relative luciferase activities in the presence of sparsomycin were shown. The renilla luciferase activities from phRL/CMV were shown for the pLuc(-1) (solid circle) and pLTRΔnefLuc (solid triangle) transfections in particular. The pLuc(-1) behaved differently from the other groups and the positive correlation between the relative luciferase activity and the concentration of sparsomycin was statistically significant (r=0.926, P<0.001, n=8, Student's t-test). The sd was within 10% from the avgerage. Shown are the representative data from two independent experiments. **(D)** Western blot analysis to measure the *Gag–Pol* and *Gag* ratio. Cell extracts were separated in the SDS-polyacrylamide gel and immunoblotted by using the rabbit polyclonal antibodies raised against p24. (lane 1, 0 nM; lane 2, 20 nM; lane 3, 200 nM; lane 4, 400 nM; lane 5, MOCK). The lower panel shows the *Gag–Pol* signal obtained from the long exposure of the same blot.

two different antibodies recognizing *Gag*. We were unable to detect a significant increase in the *Env:Gag* ratio (unpublished data), suggesting that the sparsomycin's effect on *Gag–Pol:Gag* ratio was specific. These data suggested that the translational efficiencies of viral proteins were not equally enhanced by sparsomycin. Altogether, it was strongly suggested that the sparsomycin's replication-boosting effect on HIV-1 was partly due to the enhancement of the –1 frameshift efficiency.

Discussion

In the present study, we have demonstrated that sparsomycin is an enhancer of HIV-1 replication in many human T cell lines at concentrations between 400–500nM. Our preliminary observation suggested that HIV-1 replication was also enhanced in primary peripheral blood monocyte culture (data not shown). Sparsomycin should be able to accelerate the study on the low-fitness HIV-1 such as drug-resistant mutants. As sparsomycin did not alter the IC_{50} of multiple antiretroviral drugs on both wt and drug-resistant HIV-1, its usage should be able to facilitate the phenotypic resistance testing of clinical isolates and as a result, benefit HIV-1-infected patients. Our observation raised an immediate concern as to whether sparsomycin-producing Streptomyces species caused an opportunistic infection in humans, which influenced AIDS progression. However, we did not find any reports suggesting so.

Sparsomycin and puromycin are the only antibiotics that can inhibit protein synthesis in bacterial, archaeal and eukaryotic cells (Ottenheijm *et al.*, 1986; Porse *et al.*, 1999). Sparsomycin has the ability to enhance the –1 frameshift in mammalian cells as well as *S. cervisiae* (Dinman *et al.*, 1997). The proposed molecular mechanism behind this ability was either through a higher affinity of the donor stem for the ribosome and slowing down the rate of the peptidyl transfer reaction, or a change in the steric alignment between donor and acceptor tRNA stems resulting in decreased peptidyl-transfer rates. Conversely, puromycin is not known to enhance the –1 frameshift in mammalian cells. At sub-toxic concentrations, puromycin was unable to enhance the HIV-1 replication (unpublished data). These data, along with the data provided in this paper, implied that the sparsomycin's unique ability to enhance the –1 frameshift might play a role in boosting the HIV-1 replication.

The maintenance of the –1 frameshift efficiency at the optimal range is critical for HIV-1 to replicate (Jacks *et al.*, 1988). Therefore, limiting *Gag–Pol* production should lead to an inhibition of viral replication because *pol* encodes enzymes essential for viral replication (Levin *et al.*, 1993). In contrast, it was also reported that increasing the *Gag–Pol* to *Gag* ratio by twofold resulted in a reduction of viral replication (Hung *et al.*, 1998; Shehu-Xhilaga *et al.*, 2001). Thus, a modest alteration of the –1 frameshift efficiency should markedly affect the replication capacity of HIV-1. Our data indicated that sparsomycin increased the efficiency of –1 frameshift by 1.3-fold, which produces a better replication capacity for HIV-1. As a result, we hypothesize that HIV-1 has a 'suboptimal' –1 frameshift efficiency. In theory, the 1.3-fold difference per one replication cycle becomes approximately 10-fold after 10 rounds of viral replication cycle because the effect accumulates exponentially. The difference should become larger when HIV-1 replicates with the slower kinetics and the replication profile is monitored over a longer time course. In fact, our experimental data were in good agreement with the above estimation. In nature, HIV-1 does not accumulate mutations within the frameshift signal to achieve the higher frameshift efficiencies. This implies that there are multiple and complex regulatory mechanisms that keep the efficiency of the –1 frameshift at suboptimum. Under these conditions, the best efficiency of HIV-1 survival in the host might be achieved. Altogether, one of the possible mechanisms that sparsomycin boosted the HIV-1 replication could be the enhancement of the –1 frameshift efficiency.

Acknowledgements

We thank Drs Hironori Sato and Tsutomu Murakami for critical reading of the manuscript. This work was partly supported by both the Japan Health Science Foundation and the grant from Japanese Ministry of Health, Labor, and Welfare.

References

Ash RJ, Fite LD, Beight DW & Flynn GA (1984) Importance of the hydrophobic sulfoxide substituent on nontoxic analogs of sparsomycin. *Antimicrobial Agents and Chemotherapy* 25:443–445.

Boden D, Hurley A, Zhang L, Cao Y, Guo Y, Jones E, Tsay J, Ip J, Farthing C, Limoli K, Parkin N & Markowitz M (1999) HIV-1 drug resistance in newly infected individuals. *Journal of the American Medical Association* 282:1135–1141.

Devereux HL, Emery VC, Johnson MA & Loveday C (2001) Replicative fitness *in vivo* of HIV-1 variants with multiple drug resistance-associated mutations. *Journal of Medical Virology* 65:218–224.

Dinman JD, Ruiz-Echevarria MJ, Czaplinski K & Peltz SW (1997) Peptidyl-transferase inhibitors have antiviral properties by altering programmed -1 ribosomal frameshifting efficiencies: development of model systems. *Proceedings of the National Academy of Sciences of the United States of America* 94:6606–6611.

Dulude D, Baril M & Brakier-Gingras L (2002) Characterization of the frameshift stimulatory signal controlling a programmed -1 ribosomal frameshift in the human immunodeficiency virus type 1. *Nucleic Acids Research* 30:5094–5102.

Gehringer H, Bogner JR, Goebel FD, Nitschko H & von der Helm K (2000) Sequence analysis of the HIV-1 protease coding region of 18 HIV-1-infected patients prior to HAART and possible implications on HAART. *Journal of Clinical Virology* 17:137–141.

Hertogs K, de Bethune MP, Miller V, Ivens T, Schel P, Van Cauwenberge A, Van Den Eynde C, Van Gerwen V, Azijn H, Van Houtte M, Peeters F, Staszewski S, Conant M, Bloor S, Kemp S, Larder B & Pauwels R (1998) A rapid method for simultaneous detection of phenotypic resistance to inhibitors of protease and reverse transcriptase in recombinant human immunodeficiency virus type 1 isolates from patients treated with antiretroviral drugs. *Antimicrobial Agents and Chemotherapy* 42:269–276.

Hirsch, MS, Brun-Vezinet F, D'Aquila RT, Hammer SM, Johnson, VA, Kuritzkes DR, Loveday C, Mellors JW, Clotet B, Conway B, Demeter LM, Vella S, Jacobsen DM & Richman DD (2000) Antiretroviral drug resistance testing in adult HIV-1 infection: recommendations of an International AIDS Society-USA Panel. *Journal of the American Medical Association* 283:2417–2426.

Hung M, Patel P, Davis S & Green SR (1998) Importance of ribosomal frameshifting for human immunodeficiency virus type 1 particle assembly and replication. *Journal of Virology* 72:4819-4824.

Iga M, Matsuda Z, Okayama A, Sugiura W, Hashida S, Morishita K, Nagai Y & Tsubouchi H (2002) Rapid phenotypic assay for human immunodeficiency virus type 1 protease using *in vitro* translation. *Journal of Virological Methods* 106:25–37.

Jacks T, Power MD, Masiarz FR, Luciw PA, Barr PJ & Varmus HE. (1988) Characterization of ribosomal frameshifting in HIV-1 gag-pol expression. *Nature* 331:280–283.

Jarmy G, Heinkelein M, Weissbrich B, Jassoy C & Rethwilm A (2001) Phenotypic analysis of the sensitivity of HIV-1 to inhibitors of the reverse transcriptase, protease, and integrase using a self-inactivating virus vector system. *Journal of Medical Virology* 64:223–231.

Kantor R, Fessel WJ, Zolopa AR, Israelski D, Shulman N, Montoya JG, Harbour M, Schapiro JM & Shafer RW (2002) Evolution of primary protease inhibitor resistance mutations during protease inhibitor salvage therapy. *Antimicrobial Agents and Chemotherapy* 46:1086–1092.

Kellam P & Larder BA (1994) Recombinant virus assay: a rapid, phenotypic assay for assessment of drug susceptibility of human immunodeficiency virus type 1 isolates. *Antimicrobial Agents and Chemotherapy* 38:23–30.

Komano J, Miyauchi K, Matsuda Z & Yamamoto N (2004). Inhibiting the Arp2/3 Complex limits infection of both intracellular mature vaccinia virus and primate lentiviruses. *Mol Biol Cell* 15:5197–5207.

Levin JG, Hatfield DL, Oroszlan S & Rein A (1993) Mechanisms of translational suppression used in the biosynthesis of reverse transcriptase. In *Reverse transcriptase*, pp. 5–31. Edited by AM Skalka & SP Goff. New York: Cold Spring Harbor Laboratory Press.

Matsuda Z, Yu X, Yu QC, Lee TH & Essex M (1993) A virion-specific inhibitory molecule with therapeutic potential for human immunodeficiency virus type 1. *Proceedings of the National Academy of Sciences of the United States of America* 90:3544–3548.

Menzo S, Rusconi S, Monachetti A, Colombo MC, Violin M, Bagnarelli P, Varaldo PE, Moroni M, Galli M, Balotta C & Clementi M (2000) Quantitative evaluation of the recombinant HIV-1 phenotype to protease inhibitors by a single-step strategy. *AIDS* 14:1101–1110.

Miyauchi K, Komano J, Yokomaku Y, Sugiura W, Yamamoto N & Matsuda, Z (2005) Role of the specific amino acid sequence of the membrane-spanning domain of human immunodeficiency virus type 1 in membrane fusion. *Journal of Virology* 79:4720–4729.

Nakajima N, Enomoto T, Watanabe T, Matsuura N & Ubukata M. (2003) Synthesis and activity of pyrimidinylpropenamide antibiotics: the alkyl analogues of sparsomycin. *Bioscience, Biotechnology, and Biochemistry* 67:2556–2566.

Ottenheijm HC, van den Broek LA, Ballesta JP & Zylicz Z (1986) Chemical and biological aspects of sparsomycin, an antibiotic from Streptomyces. *Progress in Medicinal Chemistry* 23:219–268.

Parkin NT, Chappey C & Petropoulos CJ (2003) Improving lopinavir genotype algorithm through phenotype correlations: novel mutation patterns and amprenavir cross-resistance. *AIDS* 17:955–961.

Pellegrin I, Breilh D, Montestruc F, Caumont A, Garrigue I, Morlat P, Le Camus C, Saux MC, Fleury HJ & Pellegrin JL (2002) Virologic response to nelfinavir-based regimens: pharmacokinetics and drug resistance mutations (VIRAPHAR study). *AIDS* 16:1331–1340.

Porse BT, Kirillov SV, Awayez MJ, Ottenheijm HC & Garrett RA (1999) Direct crosslinking of the antitumor antibiotic sparsomycin, and its derivatives, to A2602 in the peptidyl transferase center of 23S-like rRNA within ribosome-tRNA complexes. *Proceedings of the National Academy of Sciences of the United States of America* 96:9003–9008.

Rodriguez-Rosado R, Briones C & Soriano V (1999) Introduction of HIV drug-resistance testing in clinical practice. *AIDS* 13:1007–1014.

Sarmati L, Nicastri E, Parisi SG, d'Ettorre G, Mancino G, Narciso P, Vullo V & Andreoni M (2002) Discordance between genotypic and phenotypic drug resistance profiles in human immunodeficiency virus type 1 strains isolated from peripheral blood mononuclear cells. *Journal of Clinical Microbiology* 40:335–340.

Shehu-Xhilaga M, Crowe SM & Mak J (2001) Maintenance of the Gag/Gag-Pol ratio is important for human immunodeficiency virus type 1 RNA dimerization and viral infectivity. *Journal of Virology* 75:1834–1841.

Sugiura W, Matsuda Z, Yokomaku Y, Hertogs K, Larder B, Oishi T, Okano A, Shiino T, Tatsumi M, Matsuda M, Abumi H, Takata N, Shirahata S, Yamada K, Yoshikura H & Nagai Y (2002) Interference between D30N and L90M in selection and development of protease inhibitor-resistant human immunodeficiency virus type 1. *Antimicrobial Agents and Chemotherapy* 46:708–715.

Walter H, Schmidt B, Korn K, Vandamme AM, Harrer T & Uberla K. (1999). Rapid, phenotypic HIV-1 drug sensitivity assay for protease and reverse transcriptase inhibitors. *Journal of Clinical Virology* 13:71–80.

Xie D, Gulnik S, Gustchina E, Yu B, Shao W, Qoronfleh W, Nathan A & Erickson JW (1999) Drug resistance mutations can effect dimer stability of HIV-1 protease at neutral pH. *Protein Science* 8:1702–1707.

Yerly S, Kaiser L, Race E, Bru JP, Clavel F & Perrin L (1999) Transmission of antiretroviral-drug-resistant HIV-1 variants. *Lancet* 354:729–733.

Received 5 December 2005, accepted 23 March 2006

Jpn. J. Infect. Dis., 59, 77-84, 2006

Original Article

Mutations of Conserved Glycine Residues within the Membrane-Spanning Domain of Human Immunodeficiency Virus Type 1 gp41 Can Inhibit Membrane Fusion and Incorporation of Env onto Virions

Kosuke Miyauchi, Rachael Curran[1], Erin Matthews[1], Jun Komano, Tyuji Hoshino[2], Don M. Engelman[1] and Zene Matsuda*

Laboratory of Virology and Pathogenesis, AIDS Research Center, National Institute of Infectious Diseases, Tokyo 162-8640;
[2]Graduate School of Pharmaceutical Sciences, Chiba University, Chiba 263-8522, Japan; and
[1]Department of Molecular Biophysics and Biochemistry, Yale University, New Haven, Connecticut, USA

(Received December 28, 2005. Accepted January 19, 2006)

SUMMARY: The membrane-spanning domain (MSD) of HIV-1 envelope protein (Env) has an additional glycine residue within a well-conserved putative transmembrane helix-helix interaction motif, GXXXG, and forms a $G^{690}G^{691}XXG^{694}$ sequence (G, glycine; X, any residues; the numbering indicates the position within the Env of an infectious molecular clone, HXB2). Different from vesicular stomatitis virus G (VSV-G), the glycine residues of the GXXXG motif of HIV-1 showed higher tolerance against mutations, and a simultaneous substitution of G690 and G694 with leucine residues only modestly decreased fusion activity and replication capacity of HIV-1. When G691 was further substituted with alanine, phenylalanine or leucine residue while G690 and G694 were substituted with leucine residues, the efficiency of membrane fusion decreased, with the decrease greatest occurring with the leucine substitution, a less severe decrease with phenylalanine, and the least severe decrease with alanine. Substitution with leucine residue also decreased the incorporation of Env onto virions, and the mutant showed the most delayed replication profile. Thus the presence of the extra glycine residue, G691, may increase the tolerance of the other two glycine residues against mutations than VSV-G. The fact that a more severe defect was observed for the leucine residue than the phenylalanine residue suggested that the function of Env depended on the steric nature rather than on the simple volume of the side chain of the amino acid residue at position 691. Based on this result, we propose a hypothetical model of the association among MSDs of gp41, in which G^{691} locates itself near the helix-helix interface.

INTRODUCTION

The envelope protein (Env) of human immunodeficiency virus type 1 (HIV-1) is a trimer of non-covalently associated heterodimers of gp120 and gp41. As with other retroviruses, gp120 (SU) and gp41(TM) play key roles in the determination of host range and membrane fusion, respectively.

For the three subdomains of HIV-1 gp41, the structure-function relationship of the ectodomain during membrane fusion has been elucidated at the molecular level (1,2). After gp120 binds to the receptor/coreceptor, the ectodomain undergoes a conformational change to form a six-helix bundle, a common structure observed for the class I fusion protein (3,4). Information on the structure-function relationships of the membrane-spanning domain (MSD) is rather limited. Although the amino acid sequence of the MSD of HIV-1's gp41 is highly conserved among different clades, the significance of the specific amino acid sequence within MSD has been underestimated, because some heterologous MSDs can substitute functionally for the native MSD of gp41 (5,6). However, truncation of HIV-1 MSD by a glycosylphosphatidylinositol anchor abolished the fusion activity (7). Furthermore, in viruses such as simian immunodeficiency virus and the influenza virus, mutations introduced into the MSD have been shown to impede the late stage of membrane fusion (8-11). These data suggest the importance of the MSD for the function of Env.

A glycine-containing helix-helix interaction motif, a GXXXG motif, has been found in MSDs of many membrane proteins such as glycophorin A (GpA) (12,13) and the hepatitis C virus envelope glycoproteins (14). In the case of HIV-1, it occurs as a $G^{690}G^{691}XXG^{694}$ sequence (G, glycine residue; X, any amino acid residue; the number indicates the position of each glycine residue in the Env of a molecular clone HXB2 [15]) within the MSD of gp41. The glycine residues within the GXXXG motif are critical for the proper fusogenicity of vesicular stomatitis virus G (VSV-G) (16). In a previous study we have shown that the point mutations of the individual glycine residue of the GXXXG motif of gp41 MSD were well tolerated (17). The molecular basis for this high tolerance of gp41 MSD against mutations was not identified.

Here we hypothesize that the GXXXG motif of gp41, like in other transmembrane helices, forms the helix-helix interface of gp41 MSDs. We reevaluated the role of glycine residues within the gp41 MSD by introducing a simultaneous substitution of several glycine residues. We confirmed the high tolerance of gp41 MSD against mutations through the finding that any combinatorial mutations of two glycine residues with leucine residues were well tolerated. By using one of the mutants, the $LG^{691}XXL$ mutant, we evaluated the role

*Corresponding author: Mailing address: Laboratory of Virology and Pathogenesis, AIDS Research Center, National Institute of Infectious Diseases, Toyama 1-23-1, Shinjuku, Tokyo 162-8640, Japan. Tel: +81-3-5285-1111, Fax: +81-3-5285-5037, E-mail: zmatsuda@nih.go.jp

of the extra glycine residue by substituting it with several different amino acid residues, such as alanine, leucine, and phenylalanine residue. These substitutions negatively affected the function of Env, such as its fusogenicity or virion incorporation. We also found that there was a correlation between the steric characteristics of the side chain of the residue replacing G^{691} and the alteration in the function of Env. Based on these findings, we propose a potential association model of gp41 MSD.

MATERIALS AND METHODS

Construction of plasmids: The substitution mutants were generated by using the QuikChange Site-Directed Mutagenesis Kit (Stratagene, La Jolla, Calif., USA) using the subclone containing the 1.2-kb *Nhe*I-*Bam*HI fragment covering the *env* portion of HXB2RU3ΔN as described previously (17). The complementary oligonucleotide pairs used were as follow: 691F, ATGATAGTAG GATTCTTGGT AGGTTTA/ TAAA CCTACC AAGAATCCTA CTATCAT; 690/691-2L, GTACT GCTCT TGGTAGGTTT AAGAATAGTT TTTG/ CAAA AACTAT TCTTAAACCT ACCAAGAGCA GTAC; 690/694-2L, ATTCATAATG ATAGTACTGG GCTTGGTACT TTTAAG/ CTTAAAAGT ACCAAGCCCA GTACTATCAT TATGAAT; 691/694-2L, TTCATAATGA TAGTAGGACT CTTGGTACTT TTAAG/ CTTAAAAGTA CCAAGAGTCC TACTATCATT ATGAA. PCR was performed using PfuTurbo (Stratagene). The three glycine (G691) substitution mutants were created by site-directed mutagenesis using one subclone of the 2L mutants, 690/694-2L, as a PCR template and the following complementary oligonucleotide pairs: 690/694-2L + 691A, ATTCATAATG ATAGTACTGG CCTTGGTACT TTTAAG/ CTTAAAAGTA CCAAGGCCAG TACTATC ATT ATGAAT; 690/694-2L + 691L, CATAATGATA GTA CTGCTCT TGGTACTTTT AAGAAT/ ATTCTTAAAA GTACCAAGAG CAGTACTATC ATTATG; 690/694-2L + 691F, ATTCATAATG ATAGTACTGT TCTTGGTACT TTTAAG/ CTTAAAAGTA CCAAGAACAG TACTATC ATT ATGAAT). Following mutagenesis, the 1.2-kb *Nhe*I-*Bam*HI fragments were sequenced and cloned back into the pSP65HXB2RU3ΔN or pElucEnv (17) plasmid. The entire *Nhe*I-*Bam*HI portion, together with the junction, was verified by sequencing after the fragments were back.

Cells and antibodies: COS7 cells, 293 cells and 293CD4 cells (17) were grown in Dulbecco's modified essential medium (DMEM; Sigma, St. Louis, Mo., USA) supplemented with 10% fetal bovine serum (FBS) (HyClone Laboratories, Logan, Utah, USA) and penicillin-streptomycin (Gibco-BRL, Rockville, Md., USA). Jurkat cells were grown in RPMI 1640 (Sigma) supplemented with 10% FBS and penicillin-streptomycin. Cells were kept under 5% CO_2 in a humidified incubator. Anti-gp120 polyclonal antibody was obtained from Fitzgerald Industries International, Inc. (Concord, Mass., USA). The hybridoma 902 and Chessie 8 were obtained from Bruce Chesebro and George Lewis, respectively, through the AIDS Research and Reference Reagent Program, Division of AIDS, National Institute of Allergy and Infectious Diseases, National Institutes of Health (18-20). Serum from a patient infected with HIV-1 was kindly provided by T. H. Lee of Harvard School of Public Health, Boston, Mass., USA.

Protein analysis: The provirus DNA constructs were transfected into COS7 cells by electroporation or lipofection. In electroporation, COS7 cells (4 μg proviral DNA per 1×10^7 cells) were suspended in serum-free DMEM and electroporated at a 250-kV, 950-μF setting using Gene Pulsar II (Bio-Rad, Hercules, Calif., USA). In lipofection, COS7 cells (3×10^6 cells) were transfected with 7 μg proviral DNA by FuGene6 (Roche Molecular Biochemicals, Mannheim, Germany). At 72 h after transfection, transfected COS7 cells were collected by scraping and were centrifuged at 2,000 $\times$ *g* for 10 min (Allegra 6KR system; Beckman Coulter, Fullerton, Calif., USA). The cell pellets were dissolved in radioimmunoprecipitation assay (RIPA) lysis buffer (0.05 M Tris-Cl [pH 7.2] including 0.15 M NaCl, 1% Triton X-100, 1% sodium deoxycholate, and 0.1% sodium dodecyl sulfate [SDS]) and the clear lysates were centrifuged at 314,00 $\times$ *g* for 45 min at 4°C (Himac CS 120fx system; Hitachi, Tokyo, Japan). The virus was sedimented from pre-cleared supernatants (centrifuged at 2,000 $\times$ *g* for 20 min; Allegra 6KR system, then filtered through 0.45-μm-pore-size filters; Millipore, Bedford, Mass., USA) by centrifuging at 113,000 $\times$ *g* for 1.5 h at 4°C on 3 ml of a 20% sucrose cushion (SW28 rotor; Beckman Coulter). Virus pellets were dissolved in RIPA lysis buffer. Both cell and virus lysates were run on a 7.5-15% gradient in a SDS-polyacrylamide electrophoresis gel (PAGE) system (DRC, Tokyo, Japan), and proteins were blotted onto Immobilon-P (Millipore) by passive transfer, as described previously (21). The immunoblotting procedure was as described previously (17). Enhanced chemiluminescence (Roche Molecular Biochemicals) and a LAS-3000 (Fuji Photo Film, Kanagawa, Japan) were used to detect the bands.

Infection study: For the infection study, the virus seed was prepared by transfecting 1 μg of the proviral DNA into 10^6 of the COS7 cells using FuGene6 (Roche Molecular Biochemicals). Jurkat cells were infected with each virus adjusted by the p24 amount (10 ng per 10^6 cells). The infection was monitored by measuring the amount of p24 in the culture supernatant at specific time points after infection (0, 8, 15, 22 and 25 days). A p24 ELISA was performed using a p24 RETRO-TEK ELISA kit (ZeptoMetrix, Buffalo, N.Y., USA).

Flow cytometry: The level of Env expressed on the cell surface was monitored by fluorescence-activated cell sorting analysis as described previously (17). Briefly, 48 h after the COS7 cells were transfected with each Env expression vector by FuGene6, the cells were stained with the 902 monoclonal antibody for 1 h at 4°C (10 μg/ml in phosphate-buffered saline [PBS] with 2% FBS), incubated with biotin-XX goat anti-mouse immunoglobulin G (Molecular Probes, Eugene, Oreg., USA) for 30 min at 4°C, treated with streptavidin Alexa Fluor 555 (Molecular Probes) for 30 min at 4°C, and finally fixed with 1% paraformaldehyde in PBS. Cells were suspended in PBS with 2% FBS and analyzed with Becton Dickinson FACSCalibur and CellQuest software (BD Biosciences Immunocytometry Systems, San Jose, Calif., USA). A double gate was defined by forward versus side scatter and by the amount of GFP (FL-1). A total of 10,000 events within this gate were collected for analysis. An Env KO that fails to express Env was used as a negative control, as described previously (17).

T7 RNA polymerase (RNApol) transfer assay: The efficiency of fusion pore formation was examined using T7 RNApol transfer assay as described previously (17). Briefly, COS7 cells were transfected with each Env expression vector together with the reporter plasmid pTM3hRL using FuGene6. The reporter plasmid contains the T7 promoter-driven renilla luciferase. At 48 h after transfection, the transfected COS7 cells were cocultured with the 293CD4 cells

that had been transfected with the T7 RNApol expression vector, pCMMP T7RNApoliresGFP (the ratio of cells was 1:1). At 12 h after the coculture, the cells were lysed. Firefly luciferase activities, derived from the Env expression vector, and renilla luciferase activities, activated by the T7 RNApol transferred from 293CD4 cells through the generated fusion pores, were determined using the Dual-Glo luciferase reporter assay system (Promega, Madison, Wis., USA).

RESULTS

Mutagenesis of glycine residues within the GGXXG sequence: In our previous study, mutations to an individual glycine residue within gp41 MSD were well tolerated, and high tolerance of gp41 MSD against mutations was expected (17). Therefore this time we simultaneously mutated several glycine residues within the MSD (Fig. 1). First, we substituted two glycine residues with leucine residues to create three forms of 2L mutants: 690/691-2L, 690/694-2L, and 691/694-2L. In the mutant 690/694-2L, the conserved glycine residues corresponding to the GXXXG motif were substituted. A similar mutation introduced into that of VSV-G resulted in functionally defective VSV-G (16). Next, to address the significance of the additional glycine residue at position 691, we substituted G691 with alanine, phenylalanine, or leucine residue while G690 and G694 were substituted with leucine residues. These substitutions formed the 2L + 691X mutants 690/694-2L + 691A, 690/694-2L + 691F, and 690/694-2L + 691L. Thus the sequence context of 2L + 691X mutants is LXxxL (the small x represents the original sequence of HXB2). As a control, the single substitution of the G691 with phenylalanine (691F) in which the other two glycine residues were left intact was generated (Fig. 1). The single substitution of the G691 to alanine (691A) or leucine residue (691L) was well tolerated and described in our previous study as mentioned above (17).

The replication profile of the MSD mutants: To examine replication capacity, Jurkat cells were infected with the mutant viruses after the p24 amount was adjusted for. Virus replication was monitored by measuring the amount of p24 released into the culture supernatants at 0, 8, 15, 22, and 25 days after infection. A representative result of the Jurkat cell experiment is shown in Figure 2. The single substitution mutant, 691F, was replicated with a slight delay compared with the wild type (WT). Other single substitution mutants, 691A or 691L, were replicated as efficiently as the WT (described in a previous study, data not shown) (17). The 2L mutants showed slightly delayed replication kinetics compared to those of the WT. The replication of the 2L + 691X mutants was less efficient than that of the WT. Substitution with leucine residue (690/694-2L + 691L) produced the slowest replication profile in repeated experiments. These data confirmed the high tolerance of the glycine residues within the GXXXG motif of gp41 MSD against mutation. Although the replication kinetics were generally slower in the H9 cells, a similar replication profile was observed (data not shown).

WT: yikLFIMIVGGLVGLRIVFAVLSIVnrv

691F: yikLFIMIVGFLVGLRIVFAVLSIVnrv

2L mutants

690/691-2L: yikLFIMIVLLLVGLRIVFAVLSIVnrv

690/694-2L: yikLFIMIVLGLVLLRIVFAVLSIVnrv

691/694-2L: yikLFIMIVGLLVLLRIVFAVLSIVnrv

690/694-2L+691 mutants

690/694-2L+691A: yikLFIMIVLALVLLRIVFAVLSIVnrv

690/694-2L+691L: yikLFIMIVLLLVLLRIVFAVLSIVnrv

690/694-2L+691F: yikLFIMIVLFLVLLRIVFAVLSIVnrv

Fig. 1. The mutants of gp41 MSD studied. The primary structures of the MSD mutants used in this study are shown using the one-letter abbreviation of amino acid residues. The position numbering is based on that used for HXB2 Env. The portion of the predicted MSD is shown in capital letters. WT corresponds to the wild type HXB2. Mutated residues are underlined.

Analysis of the protein profiles of MSD mutants: The protein profiles of the mutants depicted in Figure 1 were examined by immunoblotting analysis using the serum from an individual infected with HIV-1 and anti-gp120 polyclonal antibody for both cell and virus lysates. Similar protein profiles were observed for all mutants and the WT in cell lysates (Fig. 3A). Almost equivalent amounts of gp160 and gp120 were observed for all constructs, and there was no obvious alteration in the processing. There was no difference found in the processing of Gag and Pol products. In the virus lysates, as in the cell lysates, no differences were found in the profiles of Gag and Pol products (Fig. 3B). However the amounts of gp120 found on 690/694-2L + 691L virions were 50-60% those of the WT (51.9% ± 14.4 %, $n = 3$, the amount of the incorporated Env was estimated by determining the ratio of the intensity of the Env to the p24 bands). This result is not due to the shedding of gp120, because the probing of the virus lysates with anti-gp41 monoclonal antibody detected a smaller amount of gp41 in 690/694-2L + 691L than in the WT (Fig. 3C). Therefore the alteration of the replication profiles observed for 690/694-2L + 691L (Fig. 2) may be accounted for by a defect in the incorporation of Env onto the virions. The reason other mutants manifested the slower replication is not evident from the protein profiles.

Fusion activity of mutants evaluated by the efficiency of fusion pore formation: Our previous study as well as others (11,17,22), have shown that mutations of the MSD sometimes negatively affect the fusogenicity of the Env. Therefore, to investigate the reason for the delayed replication observed in Figure 2, we evaluated the fusion efficiency of our mutants using the Env expression vector (Fig. 4A).

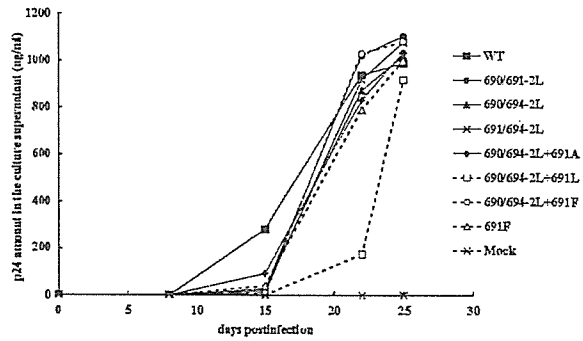

Fig. 2. The replication profile of gp41 MSD mutants in Jurkat cells. The replication of HIV-1 was monitored by measuring the p24 amount in the culture medium at 0, 8, 15, 22 and 25 days. The replication of 691A and 691L was similar to that of WT, as reported previously (17) and not shown here.

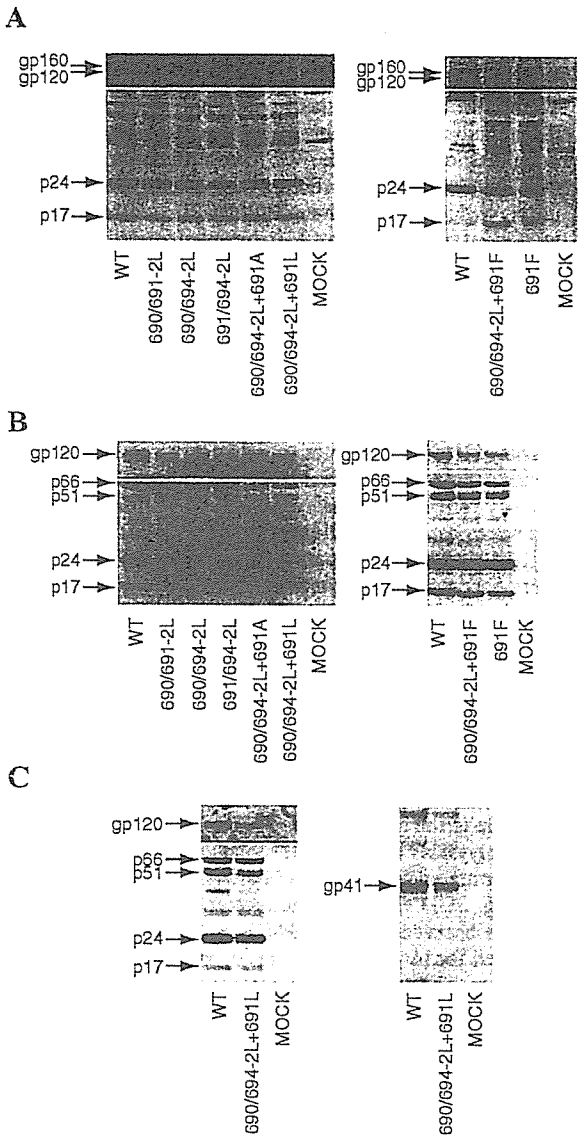

Fig. 3. Protein profiles of cell and virus lysates of the WT and mutants. The protein profiles of mutants were examined by immunoblotting. The cell (A) and virus (B, C) lysates prepared from transfected COS7 cells were used. The Env proteins (gp160, gp120 and gp41) were detected using anti-gp120 polyclonal antibody or anti-gp41 monoclonal antibody, respectively. Gag (p17 and p24) and Pol (p51 and p66) were detected using serum from an individual infected with HIV-1. The names of the mutants are shown.

First, we confirmed that the surface expression level of Env was similar by using the 902 monoclonal antibody in a flow cytometric analysis (Fig. 4B). This confirmation further supported the hypothesis that 690/694-2L + 691L has a defect in the incorporation of Env onto the virions rather than a defect in the intracellular transport of Env. We then analyzed the fusion activity of Env mutants using the T7 RNApol transfer assay. In this assay, the T7 RNApol that is transferred through the fusion pore between the Env- and receptor-expressing cells activates the T7 promoter-driven renilla luciferase. The renilla luciferase activity was normalized for transfection efficiency by the firefly luciferase activity derived from the Env expression vector. The representative data are shown in Figure 4C. Compared with WT, the 2L mutants showed a decrease in fusion efficiency of about 30%. There were no significant differences in fusogenicity among the different 2L mutants, a finding that was consistent with the replication profile shown in Figure 2. Therefore, the delayed replication observed for 2L mutants may be due to a defect in fusion. The delayed replication of 691F may also be due to a similar mechanism, although the observed decrease in the fusogenicity of 691F is not statistically significant (Fig. 4C).

The effect of the mutations of the conserved glycine residues within the GXXXG motif of gp41 MSD was less severe than in the case of VSV-G, in which a simultaneous substitution of two glycine residues corresponding to G690 and G694 resulted in almost complete elimination of fusion activity (16). The presence of an additional glycine residue within the GXXXG motif generates the GG^{691}XXG sequence in gp41 MSD, which led us to evaluate the effect of substituting other amino acid residues for the glycine residue at position 691 in the 690/694-2L context for membrane fusion. Substituting glycine residue with alanine residue did not reduce the fusion efficiency further (for example, compare 690/694-2L with 690/694-2L + 691A in Fig. 4C). However, changing the glycine residue to phenylalanine reduced the fusion efficiency significantly (690/694-2L versus 690/694-2L + 691F in Fig. 4C). The introduction of leucine residue in place of the glycine residue had the most severely negative effect. Thus the presence of a glycine residue at position 691 seems to produce an apparently higher fusion efficiency for gp41 even when the two other glycine residues constituting the GXXXG motif were replaced with leucine residue. Furthermore, because substitution with leucine resulted in less fusogenic gp41 than did substitution with phenylalanine residue, it seemed that the steric nature of the side chain at position 691, not simple bulkiness, affected the outcome.

DISCUSSION

The importance of the GXXXG motif in helix-helix association has been well established through the studies of GpA. The glycine residues within the GXXXG motif play a critical role in helix-helix interaction (13,23). Here we showed that the mutations introduced in the conserved glycine residues within the GXXXG motif of gp41 MSD were well tolerated. This finding is quite different from that of the previous study of VSV-G MSD, where a similar mutation corresponding to the 690/694-2L mutant almost abolished the fusion activity (16). Furthermore, we also observed that the substitution of any two glycine residues within the GGXXG sequence of gp41 MSD only modestly decreased the fusion activity (Fig. 4C). The expression, processing, and transport of Env proteins to the cell surface were preserved (Fig. 3A and Fig. 4B). Consistent with the modest decrease in fusion activity, the replication profiles of these mutant viruses were only slightly retarded when compared to that of the WT virus (Fig. 2). This result confirmed the high tolerance of gp41 MSD that allows the substitution of any two glycine residues within the GGXXG sequence. The results for the 690/694-2L mutant may suggest that the GXXXG motif of gp41 MSD does not play a role as a helix-helix interaction motif or that there is another mechanism that cancels out the introduced mutations.

The presence of the additional glycine residue within the GXXXG motif is a well-conserved feature of gp41's MSD (15), and this feature is absent from VSV-G. The three

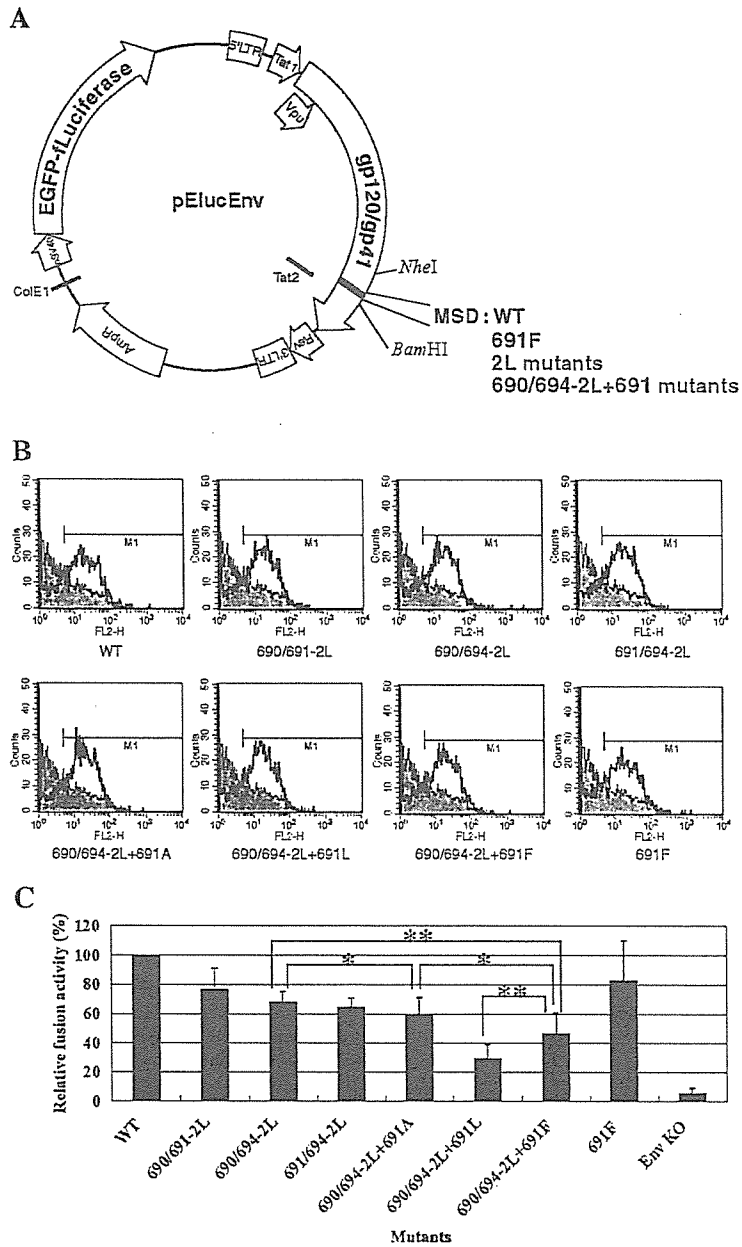

Fig. 4. Evaluation of the cell surface expression and measurement of the fusion activity of mutant Env. (A) The map of the Env expression vector, pElucEnv. pElucEnv supports the expression of HIV-1 *env* (gp120/gp41) and the gene of the EGFP-firefly luciferase (EGFP-fLuciferase) hybrid protein, respectively, from two separate promoters. The *Nhe*I and *Bam*HI sites used for cloning are indicated. The LTR, *tat*, *vpu*, and *rev* of HIV-1 are shown. AmpR, β-lactamase gene; SV40, SV40 late promoter; ColE1, ColE1 replication origin. (B) Cell-surface expression of Env. FACS analysis of Env expressed on the surface of COS7 cells transfected with each pElucEnv construct was accomplished as described in the Materials and Methods section. The signal for each Env is shown as a gray line. The filled area depicts the signal obtained for the control vector, Env KO. (C) Fusion activity of the mutants evaluated by T7 RNApol transfer assay. The cell-cell fusion assay between the Env expressing cells (containing T7 promoter-driven plasmid) and CD4+ cells (bearing the T7 RNApol expression plasmid) was used to evaluate the fusion efficiency of mutant Envs. A representative result of four independent experiments is shown (*statistically not significant, **statistically significant difference: $P < 0.05$ by Student's t test). The results shown are means ± s.d. ($n = 4$).

glycine residues will cluster within the gp41 MSD helix (Fig. 5A, prepared by the program Insight II; Accelrys, San Diego, Calif., USA). Having a hydrogen atom as its side chain, the clustering of three glycine residues may give the region more flexibility to accommodate mutations. To test whether the high tolerance of gp41MSD against mutations is attributable to the presence of the extra glycine residue within the gp41 GXXXG motif, we further mutated the extra glycine residue (G691) while the other two glycine residues were mutated to leucine residues under the $LG^{691}XXL$ context. This also allows us to obtain information on a potential helix-helix interface among gp41 MSDs. We would expect the mutation

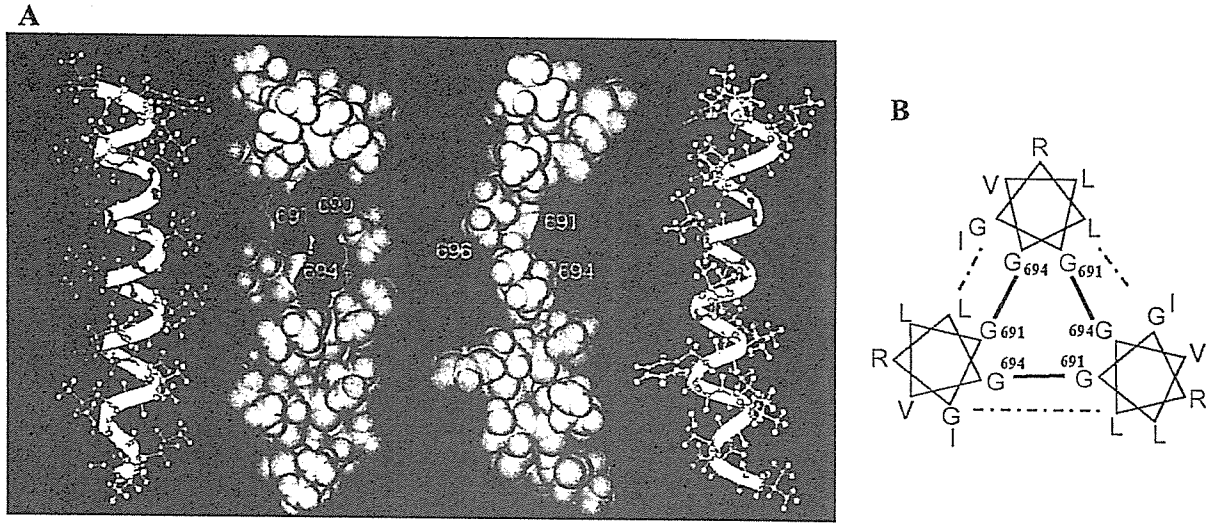

Fig. 5. A structural model of MSD and a hypothetical arrangement of the MSD helices. (A) The MSD region (position 684-705 of HXB2 Env, the amino acid sequence: LFIMIVGGLVGLRIVFAVLSIV) of the WT HXB2 was modeled in an a-helix conformation. Molecular dynamics simulations were carried out in the lipid-like environment, using the Generalized Born method with a relative permittivity of 4.0 (25, 26). The most representative structure seen in the simulation was extracted by a principal component analysis and is shown graphically. Three glycine residues (shown in red) colocalize each other and generate a hollow surface on one aspect of the helix. Two different views (ball-and-stick and CPK) of the same helix are shown. (B) A hypothetical arrangement of the MSD helices. The glycine residue at positions 691 and arginine residue at position 696 are shown in red and blue, respectively. The potential interactions between amino acid residues are shown by the bold and dotted lines, respectively.

to have no significant effect if G691 was facing outward to the lipid environment and was not involved in the helix-helix interaction. We took a genetic approach and we created the mutants 690/694-2L + 691A, 690/694-2L + 691F, and 690/694-2L + 691L. None of these mutations changed the processing or surface expression of Env (Figs. 3A and 4B). This suggests that these mutations did not induce drastic conformational changes that could be detected by a quality control mechanism of endoplasmic reticulum. Indeed, our molecular dynamics analyses of these mutants failed to detect severe deformation of the structure of the individual helix (data not shown).

When the fusion activity of the 690/694-2L + 691X mutants was evaluated, there was no statistically significant difference between glycine and alanine residue (Fig. 4C). This finding is consistent with the observation that alanine residue can functionally substitute glycine residue in transmembrane helices (23). The substitution of glycine residue with a bulky residue, namely phenylalanine residue (690/694-2L + 691F), resulted in a significant reduction in fusion activity. The fusion efficiency of 690/694-2L + 691F was about 50% that of WT. Substitution with leucine residue (690/694-2L + 691L) had an even greater negative effect on fusogenicity, and the fusion efficiency of 690/694-2L + 691L was about 30% that of WT (Fig. 4C). The replication efficiency somewhat reflected these changes in fusion activity, although we could not attribute the defect of 690/694-2L + 691L to the defect in fusion alone because 690/694-2L + 691L had an additional defect in Env incorporation (Figs. 3B and C). These results showed that the presence of glycine residue at position 691 seemed to reduce the negative effects of the leucine residue substitution of glycine residue at positions 690 and 694.

It is noteworthy that we have observed the phenotypic changes of gp41 according to the nature of the substituted amino acid residue at the position 691 (Figs. 2-4). Interestingly, the negative effect of mutations was not dependent on the mere volume of the side chain (F > L), but rather on the steric nature of the side chain. The introduction of another branched amino acid residue, isoleucine residue, at position 691 also resulted in decreased fusion activity (data not shown). This may suggest that the mutation may affect the interhelix association of MSDs, and the changes in association among MSDs may affect the function of gp41. Indeed our preliminary analysis of the measurement of helix-helix interaction by means of TOXCAT (12) analysis indicated that 690/694-2L + 691L had a slightly stronger association than WT (E. Matthews and D. M. Engelman, unpublished data). Based on these data, we present our hypothetical model of the association of the three MSDs in which the GXXXG motif is facing inward as shown in Figure 5B. Under this configuration, the G691 locates itself near the helical interface. Although this model is consistent with our observation, it places the highly conserved arginine residue downstream of the GXXXG motif toward the lipid environment. This may not be a thermodynamically favorable arrangement despite the recent finding that suggested that arginine residue can be accommodated into a lipid bilayer more easily than previously expected (24). Therefore we cannot rule out alternative arrangements of the gp41 MSDs at present. The observed high tolerance of glycines constituting this hypothetical interface may also suggest that the potential interaction among gp41 MSDs may be a rather weak one. To prove our model, the physical structure of the gp41 MSDs in lipid environments must be determined.

Here we have shown that the efficiency of the Env-mediated fusion pore formation and the incorporation of Env onto virions were affected by alterations within the MSD of gp41. This confirms that the specific primary structure of MSD is important for its proper function. Our findings also suggest that a subtle change in the structure within MSD can affect the conformations of other subdomains of gp41. Conversely, they may suggest that the conformational changes

in other subdomains may affect the structure of the MSD. This may have implications for the mechanism of disassembly and for that of uncoating events, and may also suggest that the MSD of gp41 may become another target for therapeutic intervention against HIV-1 infection.

ACKNOWLEDGMENTS

This study was supported by the Health and Labour Sciences Research Grants from Japanese Ministry of Health, Labour and Welfare.

The following reagents were obtained through the AIDS Research and Reference Reagent Program, Division of AIDS, National Institute of Allergy and Infectious Diseases, National Institutes of Health: The hybridoma 902 from Dr. Bruce Chesebro, The hybridoma Chessie 8 from Dr. George Lewis.

We are grateful to M. Segawa, H. Matsushita and H. Yamamoto for purification of the monoclonal antibodies. We thank A. M. Menting for assistance in manuscript preparation.

REFERENCES

1. Chan, D. C., Fass, D., Berger, J. M. and Kim, P. S. (1997): Core structure of gp41 from the HIV envelope glycoprotein. Cell, 89, 263-273.
2. Gallaher, W. R. (1987): Detection of a fusion peptide sequence in the transmembrane protein of human immunodeficiency virus. Cell, 50, 327-328.
3. Eckert, D. M. and Kim, P. S. (2001): Mechanisms of viral membrane fusion and its inhibition. Annu. Rev. Biochem., 70, 777-810.
4. Lu, M., Blacklow, S. C. and Kim, P. S. (1995): A trimeric structural domain of the HIV-1 transmembrane glycoprotein. Nat. Struct. Biol., 2, 1075-1082.
5. Wilk, T., Pfeiffer, T., Bukovsky, A., Moldenhauer, G. and Bosch, V. (1996): Glycoprotein incorporation and HIV-1 infectivity despite exchange of the gp160 membrane-spanning domain. Virology, 218, 269-274.
6. Deml, L., Kratochwil, G., Osterrieder, N., Knuchel, R., Wolf, H. and Wagner, R. (1997): Increased incorporation of chimeric human immunodeficiency virus type 1 gp120 proteins into Pr55gag virus-like particles by an Epstein-Barr virus gp220/350-derived transmembrane domain. Virology, 235, 10-25.
7. Salzwedel, K., Johnston, P. B., Roberts, S. J., Dubay, J. W. and Hunter, E. (1993): Expression and characterization of glycophospholipid-anchored human immunodeficiency virus type 1 envelope glycoproteins. J. Virol., 67, 5279-5288.
8. Munoz-Barroso, I., Salzwedel, K., Hunter, E. and Blumenthal, R. (1999): Role of the membrane-proximal domain in the initial stages of human immunodeficiency virus type 1 envelope glycoprotein-mediated membrane fusion. J. Virol., 73, 6089-6092.
9. Melikyan, G. B., Lin, S., Roth, M. G. and Cohen, F. S. (1999): Amino acid sequence requirements of the transmembrane and cytoplasmic domains of influenza virus hemagglutinin for viable membrane fusion. Mol. Biol. Cell, 10, 1821-1836.
10. Melikyan, G. B., Markosyan, R. M., Roth, M. G. and Cohen, F. S. (2000): A point mutation in the transmembrane domain of the hemagglutinin of influenza virus stabilizes a hemifusion intermediate that can transit to fusion. Mol. Biol. Cell, 11, 3765-3775.
11. Lin, X., Derdeyn, C. A., Blumenthal, R., West, J. and Hunter, E. (2003): Progressive truncations C terminal to the membrane-spanning domain of simian immunodeficiency virus Env reduce fusogenicity and increase concentration dependence of Env for fusion. J. Virol., 77, 7067-7077.
12. Russ, W. P. and Engelman, D. M. (1999): TOXCAT: a measure of transmembrane helix association in a biological membrane. Proc. Natl. Acad. Sci. USA, 96, 863-868.
13. Fleming, K. G. and Engelman, D. M. (2001): Specificity in transmembrane helix-helix interactions can define a hierarchy of stability for sequence variants. Proc. Natl. Acad. Sci. USA, 98, 14340-14344.
14. Op De Beeck, A., Montserret, R., Duvet, S., Cocquerel, L., Cacan, R., Barberot, B., Le Maire, M., Penin, F. and Dubuisson, J. (2000): The transmembrane domains of hepatitis C virus envelope glycoproteins E1 and E2 play a major role in heterodimerization. J. Biol. Chem., 275, 31428-31437.
15. Kuiken, C., Foley, B., Hahn, B., Marx, P., McCutchan, F., Mellors, J., Wolinsky, S. and Korber, B. (ed.) (2001): HIV Sequence Compendium 2001. Theoretical Biology and Biophysics Group, Los Alamos National Laboratory, N. Mex.
16. Cleverley, D. Z. and Lenard, J. (1998): The transmembrane domain in viral fusion: essential role for a conserved glycine residue in vesicular stomatitis virus G protein. Proc. Natl. Acad. Sci. USA, 95, 3425-3430.
17. Miyauchi, K., Komano, J., Yokomaku, Y., Sugiura, W., Yamamoto, N. and Matsuda, Z. (2005): Role of the specific amino acid sequence of the membrane-spanning domain of human immunodeficiency virus type 1 in membrane fusion. J. Virol., 79, 4720-4729.
18. Chesebro, B. and Wehrly, K. (1988): Development of a sensitive quantitative focal assay for human immunodeficiency virus infectivity. J. Virol., 62, 3779-3788.
19. Pincus, S. H., Wehrly, K. and Chesebro, B. (1989): Treatment of HIV tissue culture infection with monoclonal antibody-ricin A chain conjugates. J. Immunol., 142, 3070-3075.
20. Abacioglu, Y. H., Fouts, T. R., Laman, J. D., Claassen, E., Pincus, S. H., Moore, J. P., Roby, C. A., Kamin-Lewis, R. and Lewis, G. K. (1994): Epitope mapping and topology of baculovirus-expressed HIV-1 gp160 determined with a panel of murine monoclonal antibodies. AIDS Res. Hum. Retroviruses, 10, 371-381.
21. Matsuda, Z., Yu, X., Yu, Q. C., Lee, T. H. and Essex, M. (1993): A virion-specific inhibitory molecule with therapeutic potential for human immunodeficiency virus type 1. Proc. Natl. Acad. Sci. USA, 90, 3544-3548.
22. Armstrong, R. T., Kushnir, A. S. and White, J. M. (2000): The transmembrane domain of influenza hemagglutinin exhibits a stringent length requirement to support the hemifusion to fusion transition. J. Cell Biol., 151, 425-437.
23. Kleiger, G., Grothe, R., Mallick, P. and Eisenberg, D. (2002): GXXXG and AXXXA: common alpha-helical interaction motifs in proteins, particularly in extremophiles. Biochemistry, 41, 5990-5997.
24. Hessa, T., Kim, H., Bihlmaier, K., Lundin, C., Boekel, J., Andersson, H., Nilsson, I., White, S. H. and von Heijne, G. (2005): Recognition of transmembrane helices by the